Crust and Upper Mantle Structure in Northeastern Japan Derived from the Velocity and Azimuth Anomalies Observed at the Kitakami Seismic Array

Tôhoku Geophys. Journ. (Sci. Rep. Tôhoku Univ., Ser. 5), Vol. 29, No. 1, pp. 1–40, 1982.

Crust and Upper Mantle Structure in the Northeastern Japan Derived from the Velocity and Azimuth Anomalies Observed at the Kitakami Seismic Array

AKIRA YAMAMOTO

Observation Center for Earthquake Prediction,
Faculty of Science, Tôhoku University,
Sendai, 980

TOSHIO KONO

Kitakami Seismological Observatory, Faculty of Science,
Tôhoku University, Tono, 028-05

(Received April 27, 1982)

Abstract: More than 2500 values of apparent velocities and directions of wave approach of the earthquakes which occurred in and near the Tohoku district have been derived from the data at the Kitakami seismic array. The directions of wave approach were compared with the directions to epicenter determined from the seismic network of Tôhoku University. The smallest values of the apparent velocities which provide us the information on the value of the velocity of each layer were compared with the velocities estimated by the previous workers. In the case of the earthquakes having occurred in the east side of the array the observed anomalies in directions of wave approach and apparent velocities showed the period functions of the direction to epicenter. On the assumption that the sources of these anomalies are dipping interfaces, the dip angles and dip directions were estimated. Around the Sanriku coastal line the Conrad discontinuity has a dip angle of 7° and a dip direction of N85°W, and the Moho has a dip angle of 11° and the same dip direction as the Conrad. In the inland of the Tohoku district the Conrad is almost flat and the Moho seems to be nearly flat.

1. Introduction

In order to investigate seismic activities in and around the Japan trench (especially off the Sanriku coast) the Kitakami seismological observatory (KGJ) was constructed. KGJ is a seismic array composed of 13 stations as shown in Fig. 1 and Table I. Each observation vault is in the granites which are distributed in the Tono region, the central part of the Kitakami mountain range. The length of the vault is 50 m and the height difference between the floor and the ground surface is about 30 m on the average. A vertical component seismometer (T_0=1.0 s) is set at each station. Two horizontal component seismometers (T_0=1.0 s) are set at KM (the central station), KT, MN, OD, respectively (see Fig. 1). The simplified system of data transmission and recording is shown in Fig. 2. The details of the system are reported by Suzuki *et al.* (1972). The preliminary observation started in September 1970 and its full operation was started in November 1971.

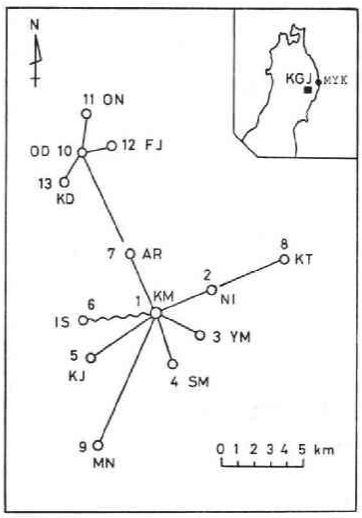

Fig. 1. Configuration of the Kitakami seismic array.
MYK is Miyako.

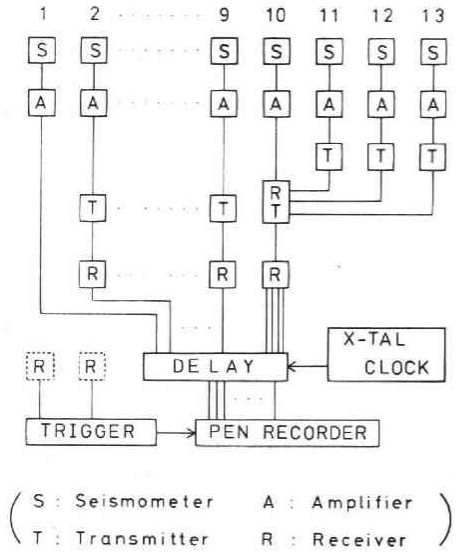

Fig. 2. Simplified system of data transmission and recording.

Table I. Coordinate of array station

No	Station	Code	X km	Y km	Z m
1	Komagi*	KM	0.000	0.000	376
2	Nishinai	NI	3.417	1.366	431
3	Yamasaki	YM	2.686	−1.342	346
4	Shimotochinai	SM	1.017	−3.133	289
5	Kokoji	KJ	−4.003	−2.830	477
6	Ishipane	IS	−4.456	−0.495	463
7	Arakawa	AR	−1.641	3.510	363
8	Kotohata	KT	7.830	3.300	554
9	Monomiyama	MN	−3.551	−8.187	488
10	Ooide	OD	−4.673	9.724	466
11	Oonodaira	ON	−4.373	12.125	616
12	Fujikirizawa	FJ	−2.841	10.187	527
13	Koide	KD	−5.754	7.870	534

* Central station (39°23′11.9″N, 141°33′56.1″E), X: the east direction, Y: the north direction

For array methods the directions of wave approach and apparent velocities are basic quantities. Generally both directions of wave approach and apparent velocities not only depend on locations of epicenter and focal depths but also are influenced by velocity structures where seismic waves propagate (*e.g.* existence of dipping boundaries). In most cases the directions of wave approach and apparent velocities deviate from the the values which are expected from horizontally layered structures.

In this study the azimuth anomaly is the difference between the direction of wave approach and the direction to epicenter, and the velocity anomaly is the difference

between apparent velocity and the expected $d\Delta/dT$ obtained from a standard velocity structure.

The purpose of the present work is to investigate the azimuth and velocity anomalies obtained from the KGJ seismic array data and to infer velocity structures which occur these anomalies. This investigation is impotant in determining hypocenters from the KGJ seismic array data.

2. Method

The directions of wave approach and apparent velocities are calculated from the equations derived by Mikumo (1965) taking into consideration the height differences between the standard station and other array stations. Taking z_0-z_j as the height difference between the standard station and the other station, V_0 as P wave velocity of the surface layer, and V as an apparent velocity, the time difference Δt_j resulting from the hieght difference is

$$\Delta t_j = (z_0 - z_j)\sqrt{(1/V_0^2)-(1/V^2)} \tag{1}$$

For example, considering $V_0=5.9$ km/s, $z_0-z_j=-100$ m, and $V=10.0$ km/s, Δt_i is -0.014 s.

As seen from equation (1), the changes of Δt_i are very small except in the case of $V \fallingdotseq V_0$. If V is nearly equal to V_0, Δt_j is smaller than a unit of reading error of a first motion of the P phase. Therefore, in the right hand side of equation (2′) of Mikumo's paper $\Delta t_j' = (z_0 - z_j)\sqrt{(1/V_0^2)-(1/V_a^2)}$ was added for correction for the high difference, where V_a is the apparent velocity obtained without the correction, V_0 is the P wave velocity of the surface layer which is 5.9 km/s derived from the data of explosions around the KGJ-array as will be mentioned later.

The distribution of differences in directions of wave approach with and without the height corrections is shown in Fig. 3. The distribution of differences in

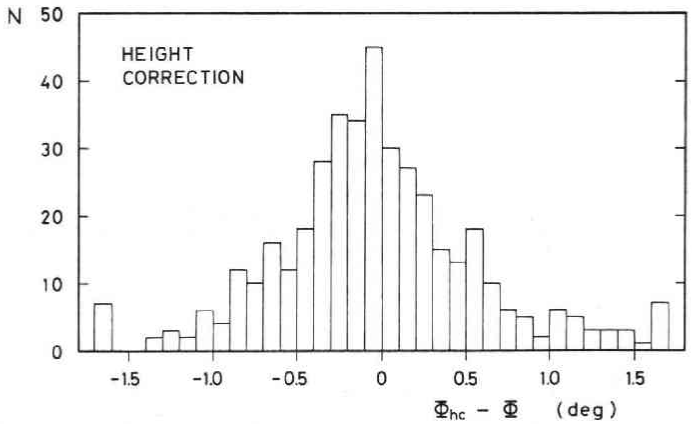

Fig. 3. Height difference effect for directions of wave approach. Φ_{hc} is a direction of wave approach with the height difference corrections. Φ is that without the height difference corrections.

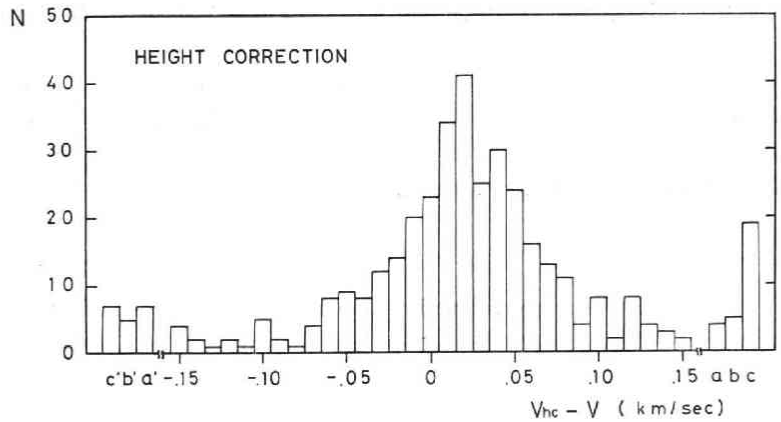

Fig. 4. Height difference effect for apparent velocity. V_{hc} is an apparent velocity with height difference corrections. V is that without height difference corrections.
a,a': $0.16 \leqq |V_{hc}-V| < 0.20$ (km/s) b,b': $0.20 \leqq |V_{hc}-V| < 0.30$ c,c': $0.30 \leqq |V_{hc}-V|$

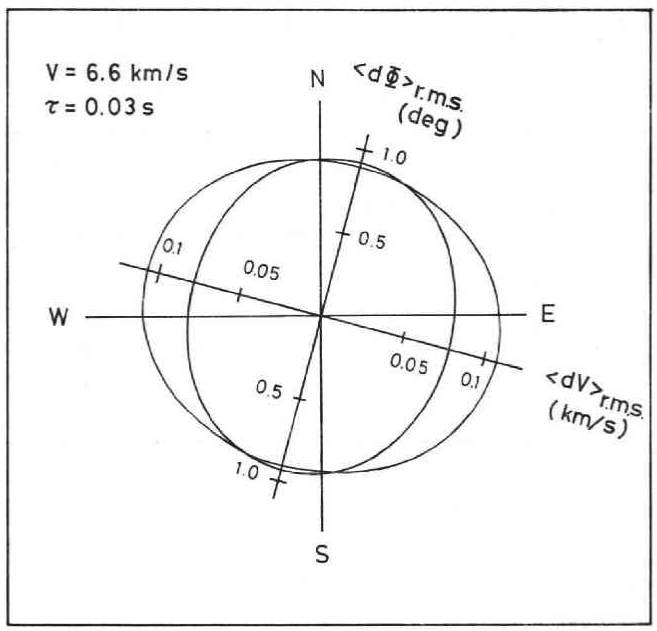

Fig. 5. Root mean squares of the errors of apparent velocity and direction of wave approach resulting from errors in reading time (Stations 1–10). τ is a standard deviation of errors in reading time.

apparent velocities with and without the height corrections is shown in Fig. 4. The differences of the directions of wave approach are predominantly distributed within $\pm 1.5°$. In the case of the apparent velocities, the differences are less than or equal to the probable errors of apparent velocities.

Readings of relative P-onset times were carried out by using the X-Y reader

whose minimum unit is 0.0254 cm. As the paper speed is 30.0 mm/s, the machinary minimum unit of reading times is smaller than 0.01 s. In the present study the errors are within ± 0.03 s, because the earthquakes whose P-onsets could be read within ± 1.0 mm were selected.

The errors in apparent velocity and direction of wave approach resulting from the errors in reading time were estimated by the same method described by Otsuka (1966). In the case of 10 stations (Stations 1–10 in Fig. 1) assuming the apparent velocity to be 6.6 km/s and the standard deviation of errors in reading time to be 0.03 s, the root mean squares of the errors in the apparent velocity and in the direction of wave approach were calculated and are shown in Fig. 5. The patterns of those errors depend on the shape of the array. In the case of the standard deviation of the errors of reading time 0.03 s and the apparent velocities 6.6, 8.0, 10.0, 12.5, and 15.0 km/s, respectively, the maxima in r.m.s. of the errors in direction of wave approach and apparent velocity are shown in Table II.

If the geometry of the array changes, the paths of the seismic waves which reach the array also vary. For this reason it is possible that the directions of wave approach and the apparent velocities are changed. The directions of wave approach and the apparent velocities obtained from the data of the above-mentioned 10 stations were compared with those calculated from the data of 13 stations. Fig. 6 shows the apparent velocities. Up to 17 km/s the differences of the apparent velocities from the 13 stations data and the 10 stations data are distributed within ± 0.2 km/s. In the case of more than 17 km/s those differences are distributed within ± 0.5 km/s which are equal to or less than the probable errors in apparent velocity. Fig. 7 shows the distribution of the differences in the direction of wave approach between the data of 10 stations and that of 13 stations. Ninety-five per cent of those differences are distributed within $\pm 2°$, and there is no systematic error between them. Therefore, in the present study the calculations were carried out by using the data from the 10 stations mentioend above. In the case of the earthquakes whose epicentral distances are less than 100 km, the average error resulting from a plane wave approximation in direction of wave approach is 2–3°, that of apparent velocity is 2–3% of the apparent velocity.

As to the main sources where propagation directions of seismic wave are deflected,

Table II. The maximum values of the root mean square errors in direction of wave approach (Φ) and apparent velocity (V) occurring from random reading errors (standard deviation of the reading erros: 0.03 s) in the case of the Kitakami seismic array (Stations 1–10).

V km/s	$<d\Phi>$ r.m.s. deg	$<dV>$ r.m.s. km/s
6.6	0.93	0.11
8.0	1.13	0.16
10.0	1.41	0.25
12.5	1.76	0.38
15.0	2.11	0.55

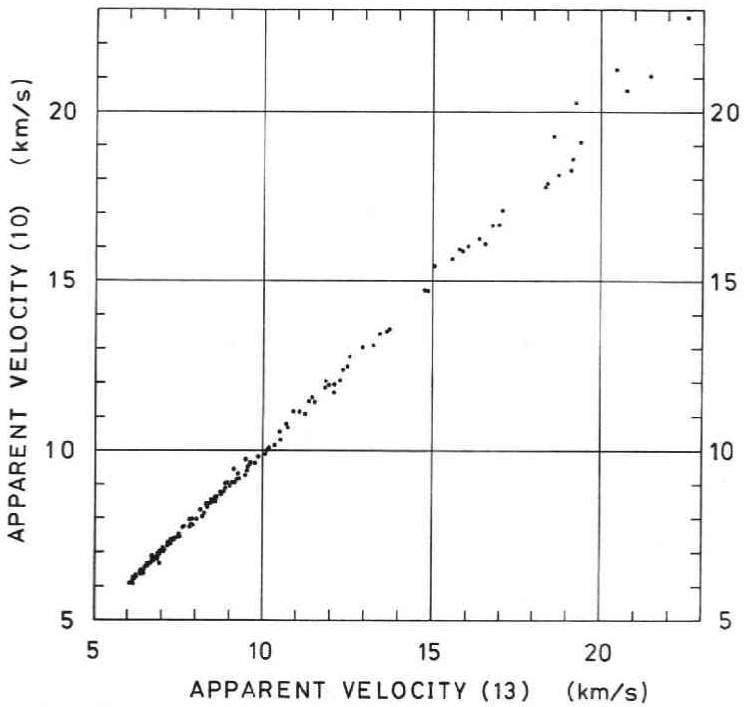

Fig. 6. Apparent velocities obtained from 10 stations versus those obtained from 13 stations.

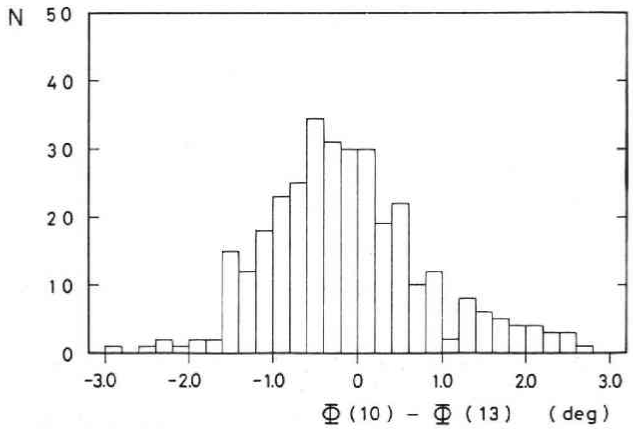

Fig. 7. Distribution of differences between directions of wave approach obtained from 10 stations and those obtained from 13 stations.

dipping interfaces and lateral inhomogeneities of velocity can be considered. In this paper the former was taken into consideration. The equations which give the amounts of deflection of seismic wave induced by a dipping interface have been derived, for example, by Matuzawa (1935) and Niazi (1966). The equations of Matuzawa (1935) were adopted. We consider one dipping interface. Let the dip angle be ω, the

velocity of the lower layer V_2, that of the upper layer V_1 ($V_2 > V_1$), the angle between the incident seismic beam and the vertical line θ, and the azimuth of the incident seismic beam measured from the dip direction anti-clockwise φ. Then the angle between the refracted seismic beam and the vertical line θ' and the azimuth of the refracted seismic beam φ' are given by

$$\cot\varphi' = \cot\varphi - \cot\varphi\sin^2\omega - \cot\theta\sin\omega\cos\omega/\sin\varphi + \sqrt{1-n^2+n^2(\sin\theta\cos\varphi\sin\omega+\cos\theta\cos\omega)^2}\,\sin\omega/(n\sin\theta\sin\varphi) \quad (2)$$

$$\cos\theta' = n\cos\theta\sin^2\omega - n\sin\theta\cos\varphi\sin\omega\cos\omega + \sqrt{1-n^2+n^2(\sin\theta\cos\varphi\sin\omega+\cos\theta\cos\omega)^2}\cos\omega \quad (3)$$

where $n=V_1/V_2$. Therefore $\varphi'-\varphi$ is the deflection of seismic rays at the interface. If V_1 is the velocity of the surface layer, θ' is an incident angle at the surface. If there is another interface above that layer, φ' is a new azimuth and θ' is a new angle between the incident seismic beam and the vertical line. It must be noted that $\varphi'-\varphi$ is the deflection at the interface but not the observed azimuth anomaly itself.

In Fig. 8 R is the station, S is the epicenter, and B is the projection of the point where the seismic ray refracts from the lower layer to the upper layer. The x- and y-axes are taken eastward and northward, respectively. Let the direction to the epicenter be γ, the direction of wave approach γ', the absolute value of the deflection of the seismic ray at B is β, and $\angle\mathrm{SRB}=\alpha$. $\alpha=|\gamma'-\gamma|$ is the absolute value of the azimuth anomaly observed at R. Considering $\triangle$BRS the following relation is obtained from the law of sine: $\sin\alpha=(\mathrm{SB}/\mathrm{SR})\sin\beta$. If α and β are small (up to about $\pi/6$), we obtain $\alpha=(\mathrm{SB}/\mathrm{SR})\beta$. Therefore, the absolute value of the observed azimuth anomaly depends on the epicentral distance, the position where the seismic ray refracts, and the amount of deflection at the refracting point. If a distance between a refraction point and a station is small, or if an epicenter and a refraction point are distant enough from the station, $\mathrm{SB}/\mathrm{SR}\fallingdotseq 1$ *i.e.* $\alpha=\beta$. In the latter case the examples of the azimuth anomalies and the apparent velocities are shown in Fig. 9(a) and (b). In Fig. 9(a) $V_1=5.9$ km/s $V_2=6.6$ km/s, $\omega=10°$, and the azimuth is measured from

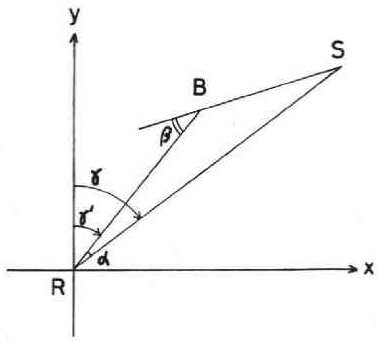

Fig. 8. Deflection (α) observed at a station (R) and that (β) occurred at a point of interface (B). S is an epicenter.

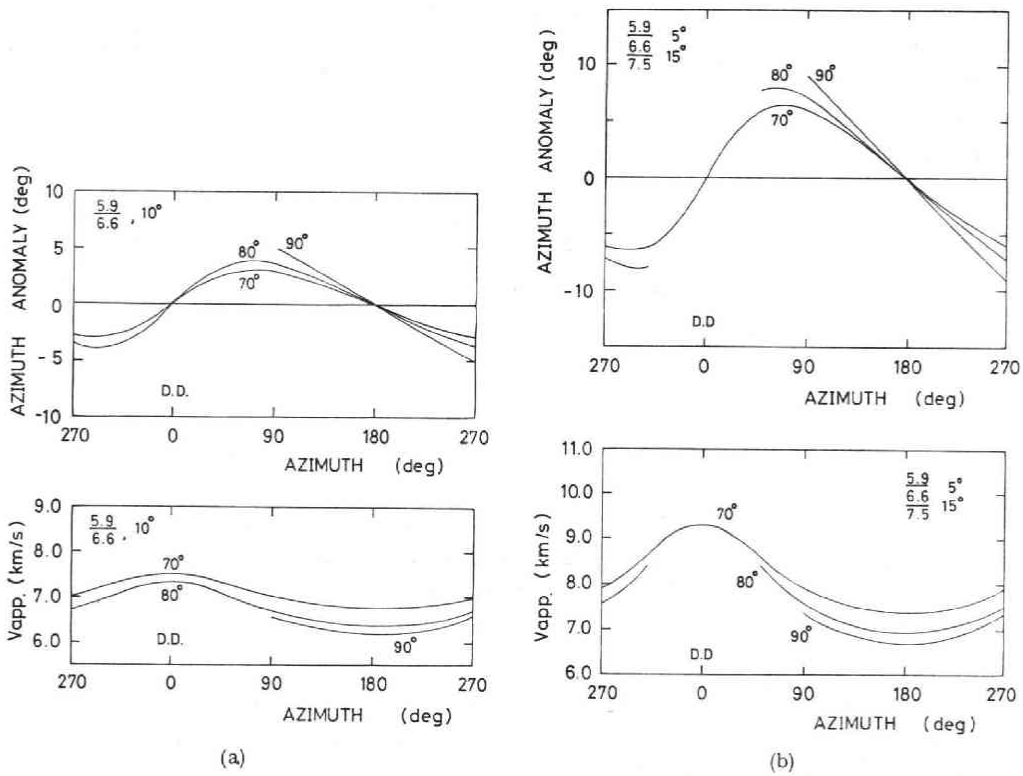

Fig. 9(a). An example of azimuth anomalies and apparent velocities from a dipping interface. Numerals on the curves are the angles between the incident seismic rays and the vertical lines at the interfaces. D.D. is a dip direction.
(b) An example of azimuth anomalies and apparent velocities by two dipping interfaces with the same dip direction.

the dip direction and is reduced in a clockwise sence. In Fig. 9(b) $V_1=5.9$ km/s, $V_2=6.6$ km/s, $\omega_1=5°$, $V_3=7.5$ km/s, $\omega_2=15°$, and both dip directions of the two dipping interfaces are coincident. The numerals above or below the curves in Fig. 9(a) and (b) are the angles between the incident seismic ray and the vertical line at the lower interface.

3. Observation results

3.1. *P wave velocity under the KGJ-array and its vicinity*

Around the KGJ-array the explosions hve been carried out at the mines and quarries. Using the data obtained from the seismic motions generated by the explosions the apparent velocities ($d\Delta/dT$) were calculated. The results are shown in Fig. 10 (a). In the case of the explosion carried out on 12 October 1975 at the Shinyama pit of the Kamaishi mine, the shot time was observed ($01^h01^m56.75^s$ JST). The relation between the arrival times (t) and the distances (Δ) is shown in Fig. 10(b). Applying the method of least squares for the data, we have

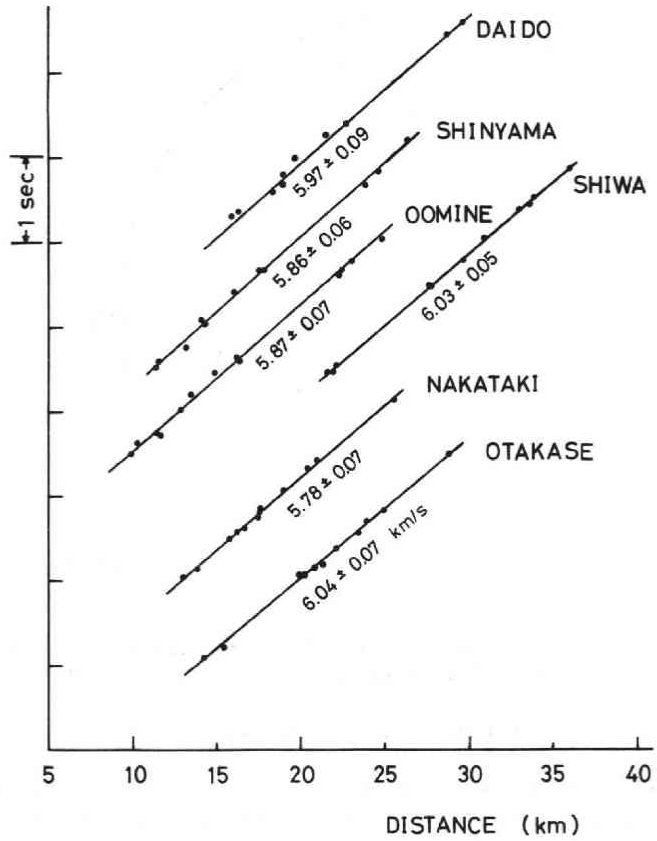

(a)

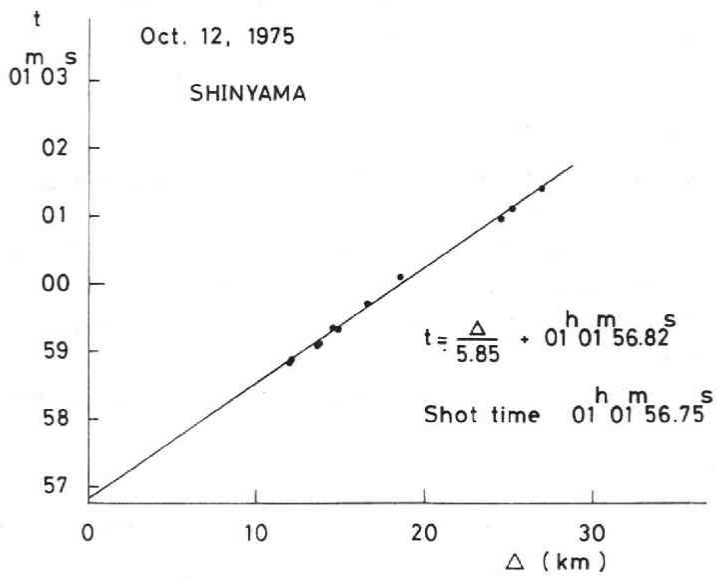

(b)

Fig. 10(a). Relative arrival times versus distances for the explosion data.
(b) Arrival times versus distances.

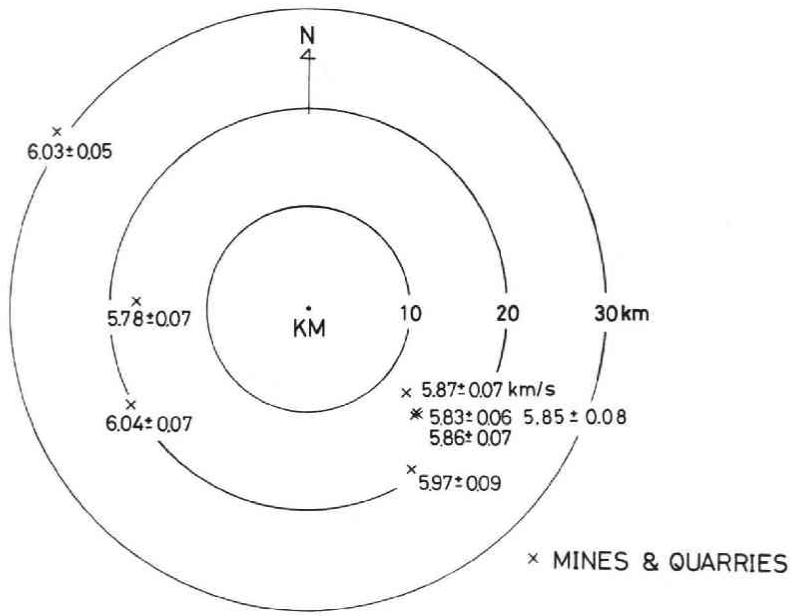

Fig. 11. Locations of shot points (the mines and the quarries) and observed apparent velocities. KM is the central station of the KGJ-array.

$$t = \{\Delta/(5.85\pm0.083)\} + 01^h\,01^m\,56.82^s \pm 0.04^s$$

The array, the shot points, and the apparent velocities are shown in Fig. 11. As the intercept time is approximately 0, it is considered that 5.9 km/s is the velocity of the surface layer under the KGJ-array. The value (5.9 km/s) agrees with both 5.92 ± 0.12 km/s obtained by Yoshii and Asano (1972) from the explosion data along the Oga-Kesennuma line and 6.0–6.1 km/s derived by Sato (1979) from data from the natural earthquakes that occurred in the inland of the Tohoku district.

3.2. *Data for apparent velocities and velocity anomalies*

The earthquakes that occurred in 1976 and satisfied the following condition were analyzed. The conditions are

1) The hypocenters are determined by the seismic network of Tôhoku University, and the standard deviations in x- and y-directions are within $\pm0.05°$.
2) The depths of the earthquakes are 0–60 km, and their standard deviations are within ±10 km.
3) When the directions of wave approach and the apparent velocities are calculated, the absolute values of the residuals in time at each station are less than 0.1 s.

3.3 *The relations between the directions to epicenter and the apparent velocities*

Hereafter we discuss the apparent velocities, azimuth anomalies, *etc.* using the directions to epicenter, the directions of wave approach, and the epicentral distances.

Therefore Fig. 12 was prepared for promptly locating the areas of interest. The relations between the directions to epicenter and the apparent velocities at intervals of 10 km depth are shown in Fig. 13(a)-(f). The epicentral distances were measured from the central station, KOMAGI, to the epicenters. Within 100 km in epicentral distance the apparent velocities approaching from the east side of the array are greater than those from the west side. This tendency is remarkable in the depth range of 10–19 km (Fig. 13(b)). In the east side of the array the smallest values of the apparent velocities change corresponding to the directions of wave approach remarkably and have the tendency to reach the minima around 90° (the east). The tendency is also notable in the case of the depth range of 20–29 km (Fig. 13(c)).

When taking into account the velocity structure of the Tohoku district (*e.g.* Yoshii and Asano (1972)) it is to be noted that the P_n phase appears as a first arrival of P wave if the epicentral distance is more than 200 km and the focus is in the crust. When the Moho discontinuity is not dipping, the epicentral distance is more than 200 km, and its depth is shallower than 60 km, the expected apparent velocity is a little more than or equal to the value of P_n. On condition that the epicentral distances are more than 200 km and the depths are shallower than 60 km, the relation between the apparent velocity and the direction of wave approach mainly in the east side of the array is shown in Fig. 14. In the case of the earthquakes that occurred around the Japan trench (off the Sanriku coast) the earthquakes with depth of more than 60 km are also plotted with open circles for the reason that will be mentioned later. The value of the apparent velocity reaches a minimum at about 90° (the east) in the

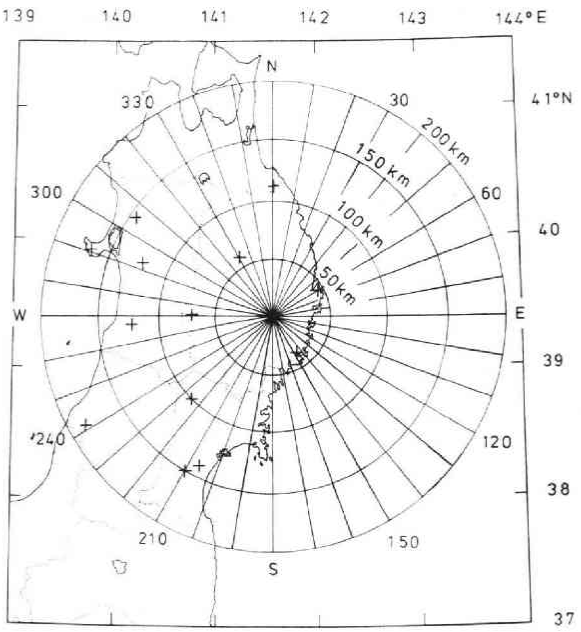

Fig. 12. Map showing the distances and the azimuths. The center is the Komagi station (KM). The crosses are the stations of the seismic network of Tôhoku University in 1976.

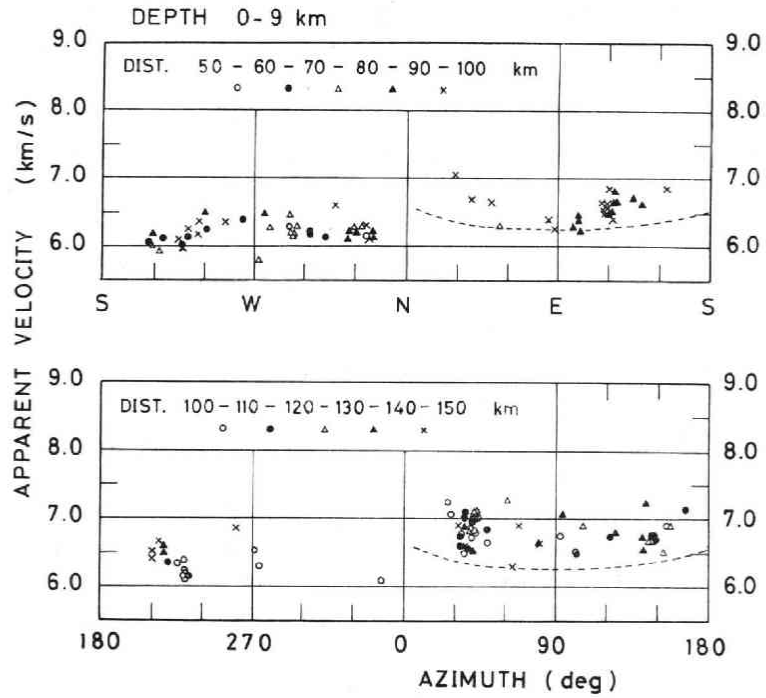

Fig. 13(a)

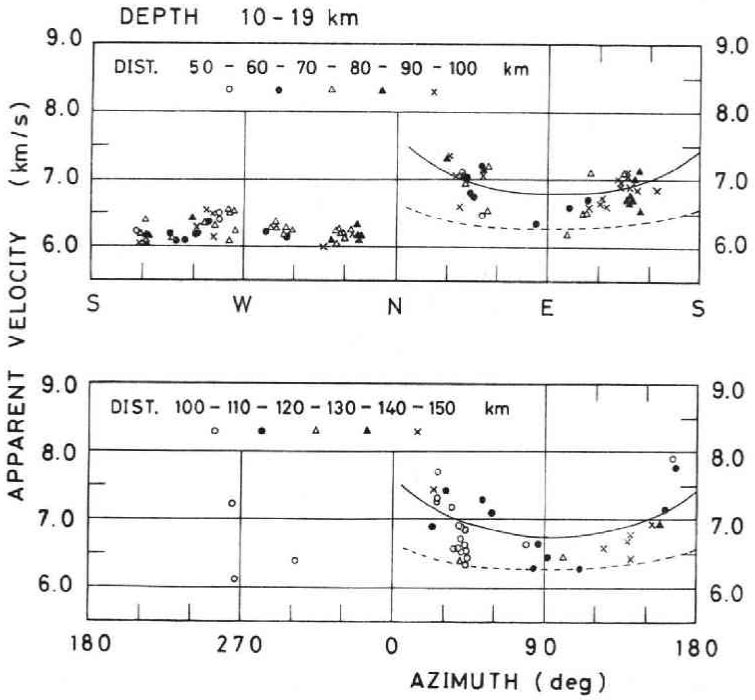

Fig. 13(b)

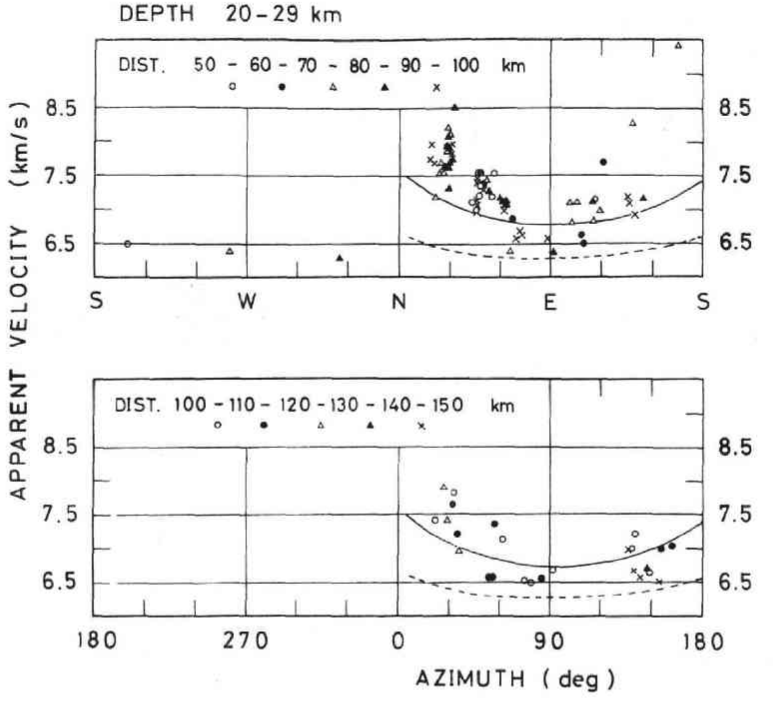

Fig. 13(c)

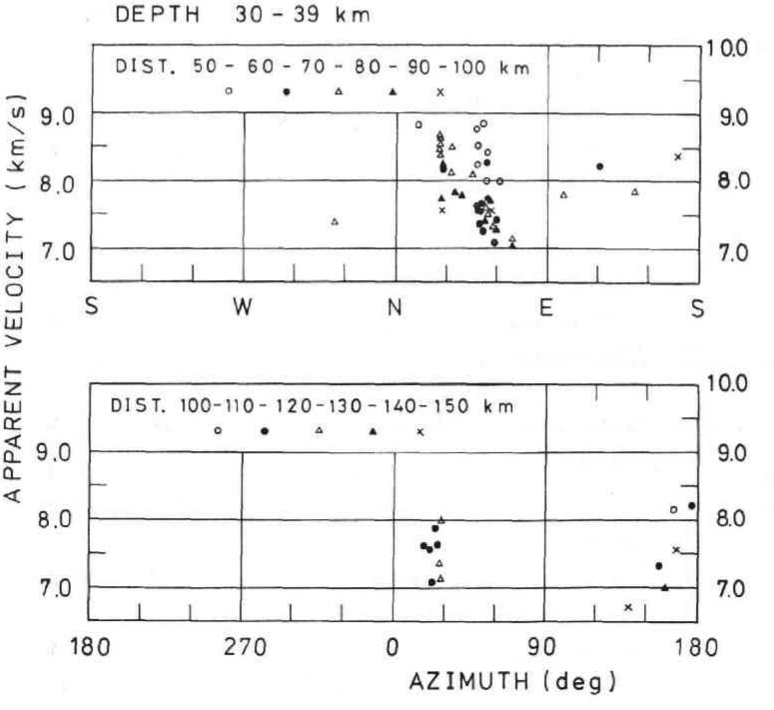

Fig. 13(d)

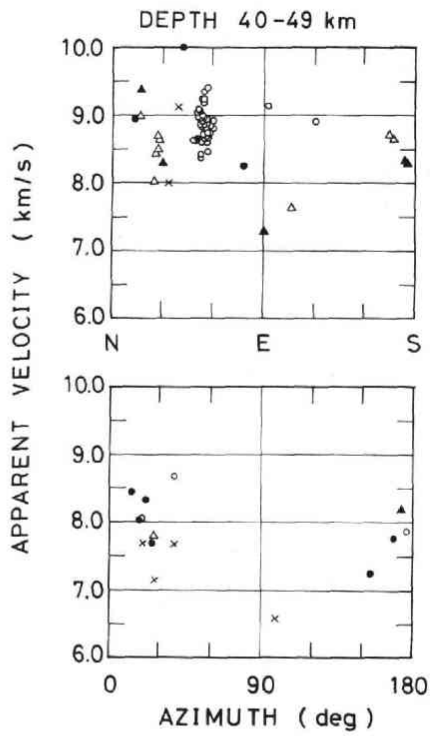

Fig. 13(e)

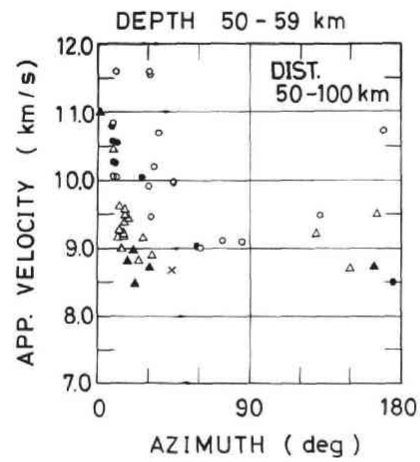

Fig. 13(f)

Fig. 13 (a)-(f). Apparent velocities versus directions to epicenter. The dotted line represents the apparent velocities from the following condition: The dip direction of the interface between the 5.9 km/s layer and the 6.6 km/s layer is N85°W, the dip angle is 7°, and the angle between the incident seismic ray and the perpendicular line at the interface is 90°. The solid line shows the apparent velocities from the following condition: Under the same velocity structure mentioned above the Moho has the same did direction and a dip angle of 11°.

direction to the epicenter, and at about 0° (the north) and about 180° (the south) the lower limit of the apparent velocities is about 7.5 km/s. This value agrees with the values of P_n in the Tohoku district obtained by Yoshii and Asano (1972) (7.5 km/s) and RGES (1977) (7.53±0.53 km/s).

3.4. *The relation between the epicentral distances and the apparent velocities*

In the investigation of the earthquakes that occurred in the easterly direction of the array and their epicentral distances are more than 150 km, the data on the earthquakes whose standrd deviations in latitude and longitude 0.05°–0.07° and those in depth 10–30 km were also included. The relations between the apparent velocities and the epicentral distances (classified by the azimuth range) are shown in Fig. 15(a)-(q). In the Figure when the numerals which show the depths are in brackets, the earthquakes with epicentral distances of more than 150 km and the depths of not greater than 60 km are included. In the case of the earthquakes that occurred around the Japan trench,

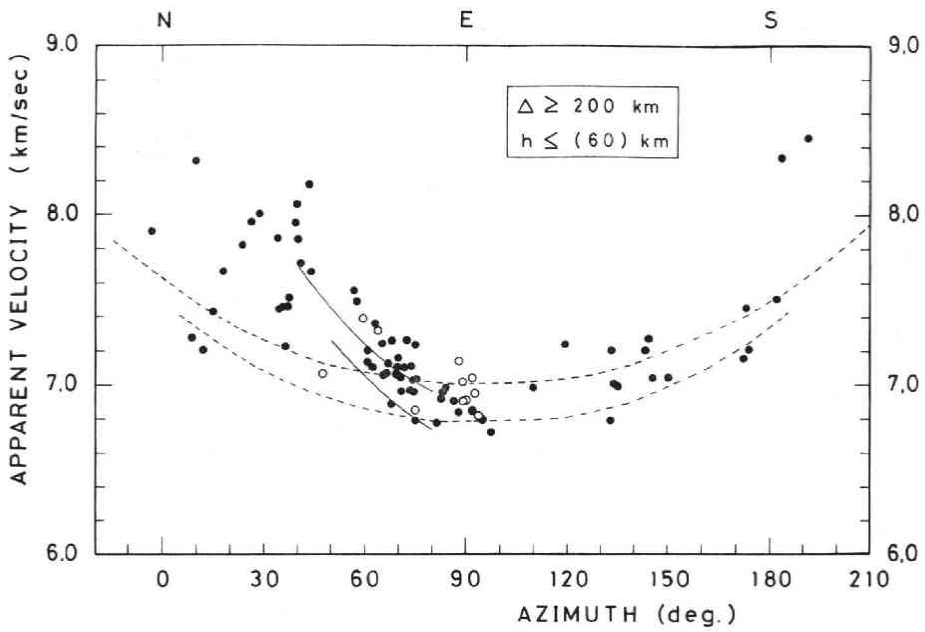

Fig. 14. Apparent velocities versus directions to epicenter. The epicentral distance is 200 km or more and the focal depth range is 0–60 km (solid circles). The open circles represent the cases in which the depths of the earthquakes occurred around the Japan trench were determined to be more than 60 km by the seismic network of Tôhoku University. The dotted lines represent the same apparent velocities mentioned as in Fig. 13. The solid lines show the apparent velocities under the following condition: Both dip directions of the Conrad and the Moho are N50°W, and their dip angles are 15° and 20°, respectively, and the angles between the incident seismic ray and the vertical line at the Moho are 90° (the lower dotted and solid lines) and 80° (the upper dotted and solid lines).

no limitation of depth is made as will be described later. The vertical bars indicate the limit of the standard deviation in apparent velocity. In the case of the earthquakes that occurred in the easterly direction of the array the patterns of the relation between apparent velocity and epicentral distance change depending on the azimuth range. This implies that the velocity structure under the array and its surrounding area is complex.

In the case of the earthquakes that occurred in the westerly direction of the array the depths of those earthquakes are less than 20 km except for a few events. The relations between the epicentral distances and apparent velocities have the pattern which has jumps of the lower limit values of the apparent velocities at some epicentral distances. In general, the constant lower limit value of the apparent velocity in some epicentral distance range is considered to correspond to the velocity of layer.

3.5. *Depths and apparent velocities*

In the case that the epicenters are in a small area the apparent velocities increase as the depth increases. Let us consider two regions (41–42°N, 140–143°E) and (37–38°N, 139–142°E). In these regions the epicentral distances are distributed in the

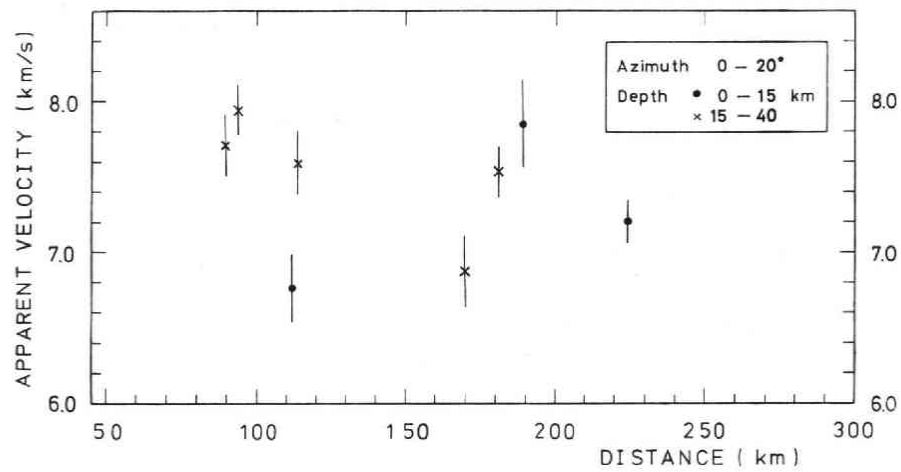

Fig. 15 (a)

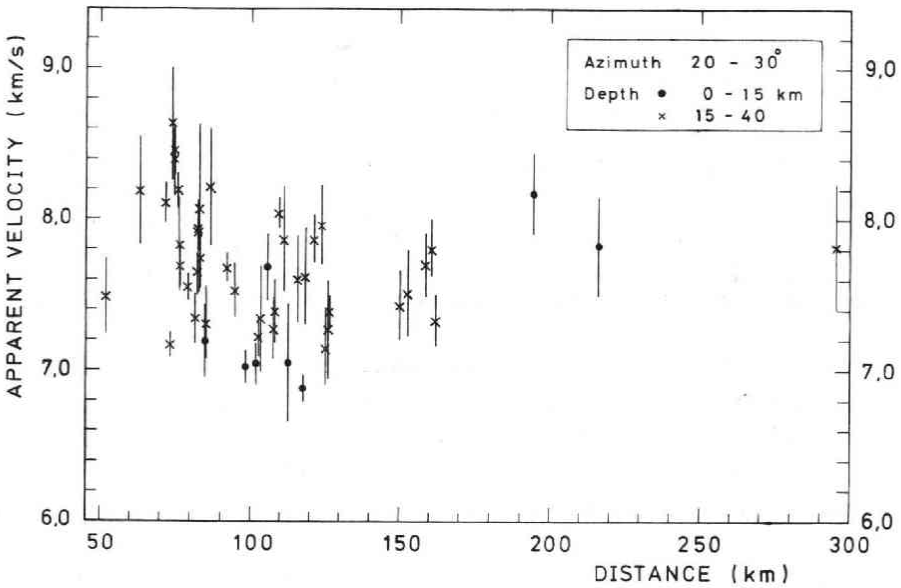

Fig. 15 (b)

range 200–300 km. The earthquakes having occurred in these regions from January 1972 to December 1975 were investigated. As to the earthquakes whose hypocenters were determined by JMA, the relations between depths and apparent velocities are shown in Fig. 16(a) and (b). In the Figure the solid lines correspond to the values of $d\Delta/dT$ (at Δ=200 km) obtained from the velocity structure adopted by Tôhoku University. Setting aside the values of apparent velocities, we can see that the apparent velocity increases as the depth increases. In regard to the earthquakes which occurred in the same regions from April 1975 to December 1975 and whose hypocenters were determined

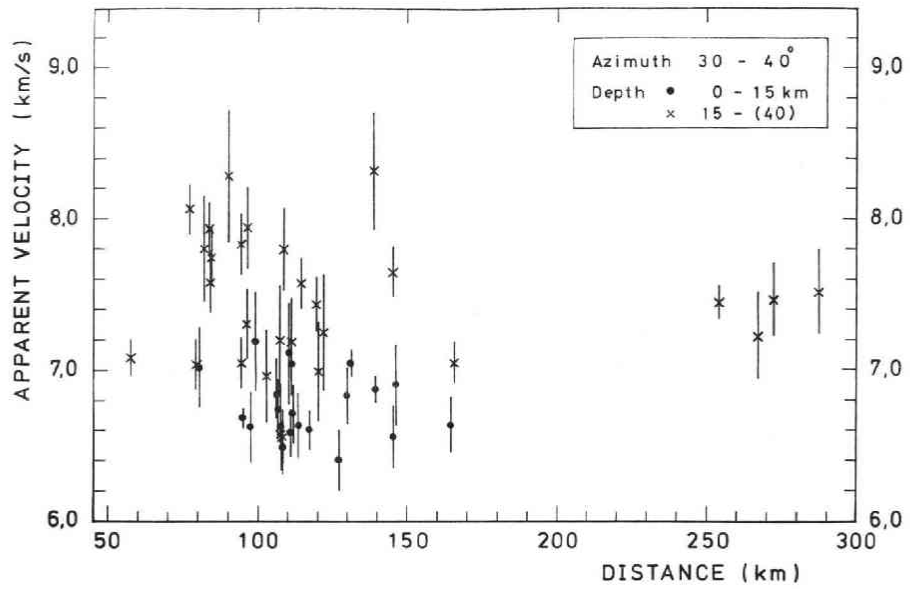

Fig. 15 (c)

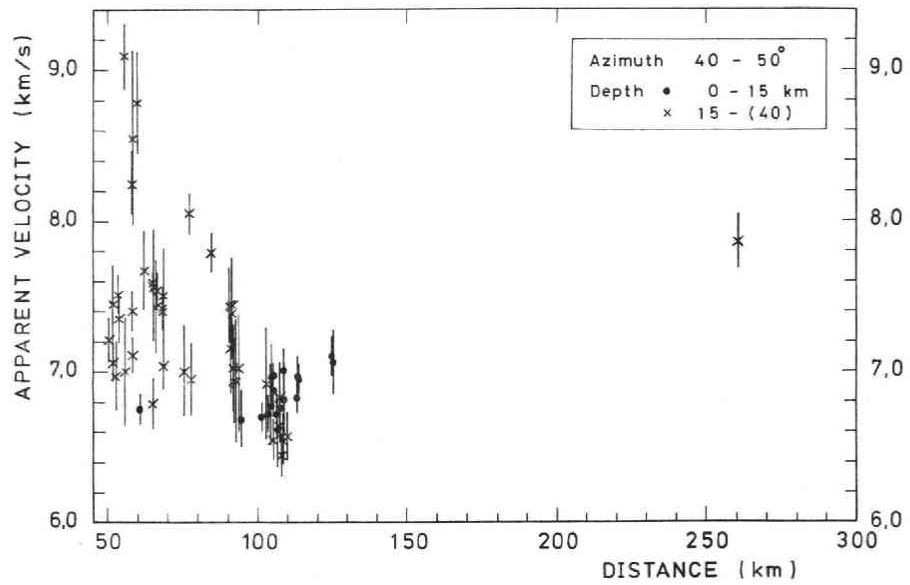

Fig. 15 (d)

by Tôhoku University, the relations between depths and apparent velocities are plotted in Fig. 16(c) and (d). There are good correlations between the apparent velocities and the depths in spite of the locations of the regions being outside the seismic network of Tôhoku University.

Let consider the Japan trench region (39–40°N, 144–145°E). This region is

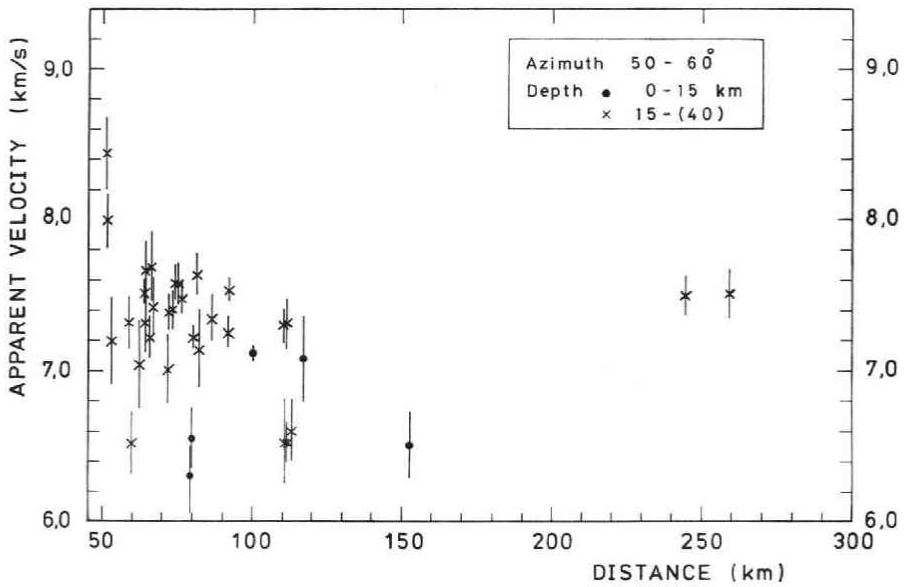

Fig. 15 (e)

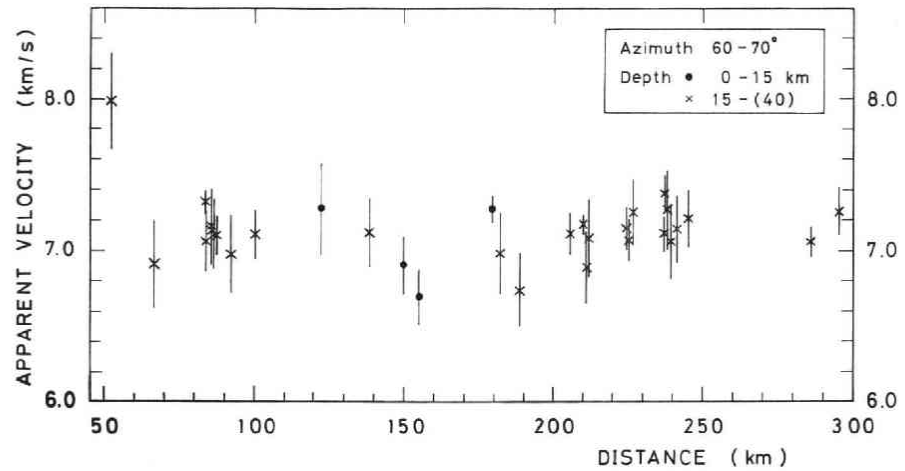

Fig. 15 (f)

located in almost the same epicentral distance range as the two regions mentioned above but very far from the seismic network of Tôhoku University. The relation between the depth and the epicentral distance is shown in Fig. 16(e). The solid line is the same as in Fig. 16(a). The dotted line indicates $d\Delta/dT$ which are obtained under the following conditions. 1) the thickness of the 5.9 km/s layer is 10 km and that of the 6.6 km/s layer is 20 km in the parallel region. 2) the interface between the 5.9 km/s layer and the 6.6 km/s layer and that between the 6.6 km/s layer and the 7.5 km/s layer (the Moho) have the same dip direction (N90°W). The dip angle of the former is 5°

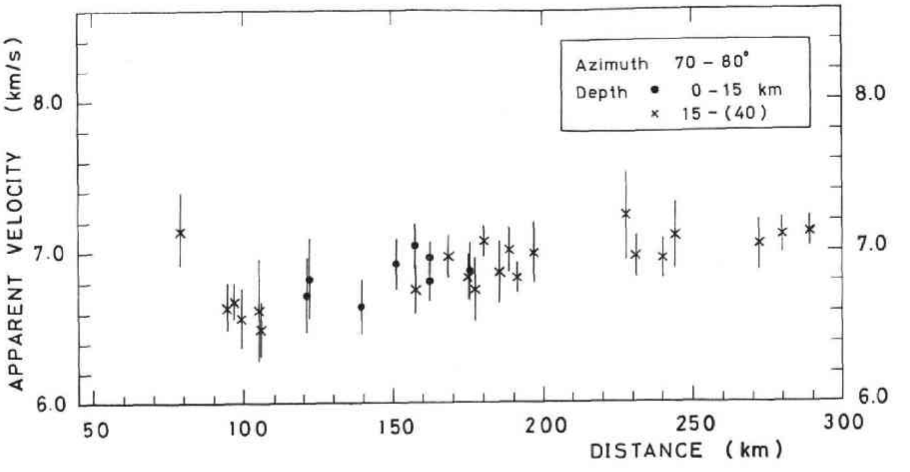

Fig. 15 (g)

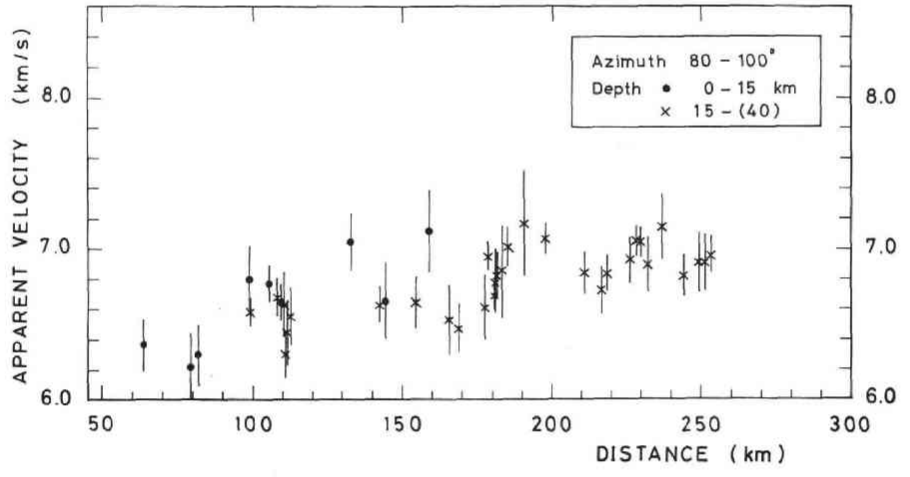

Fig. 15 (h)

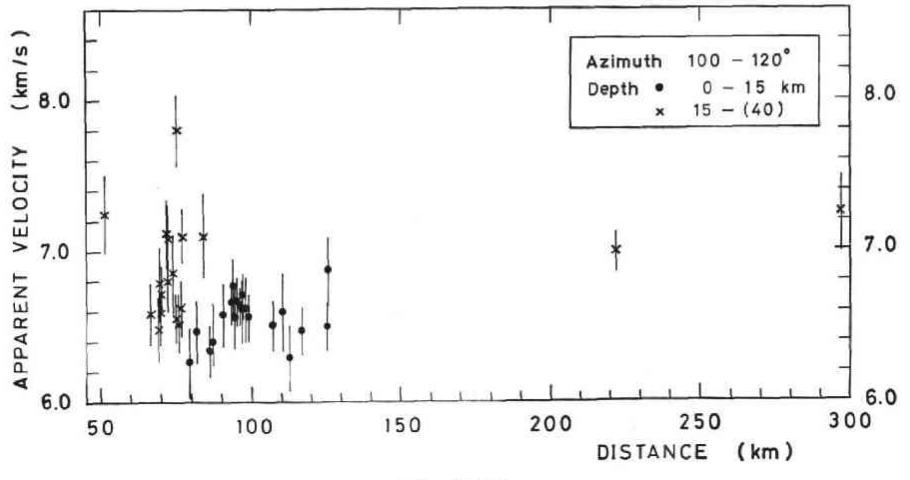

Fig. 15 (i)

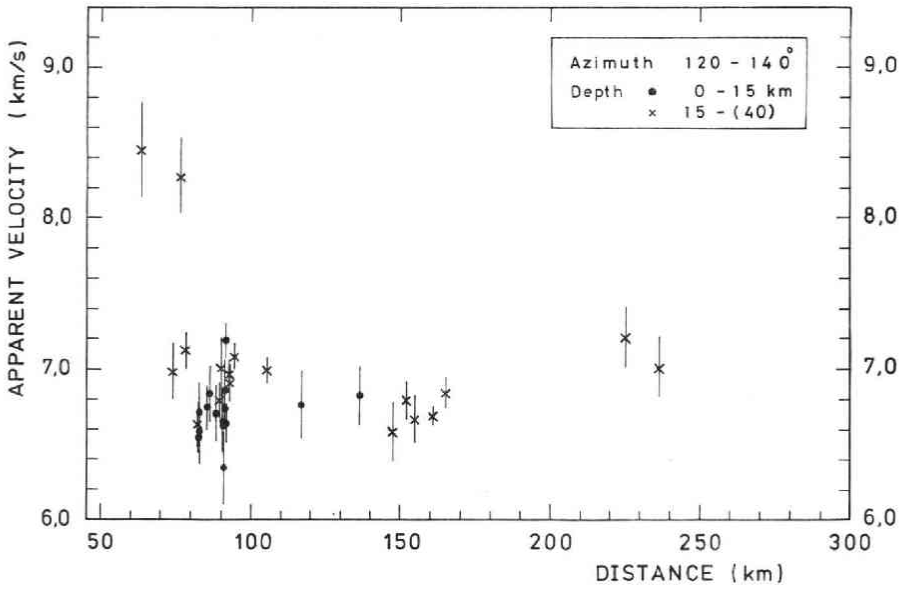

Fig. 15 (j)

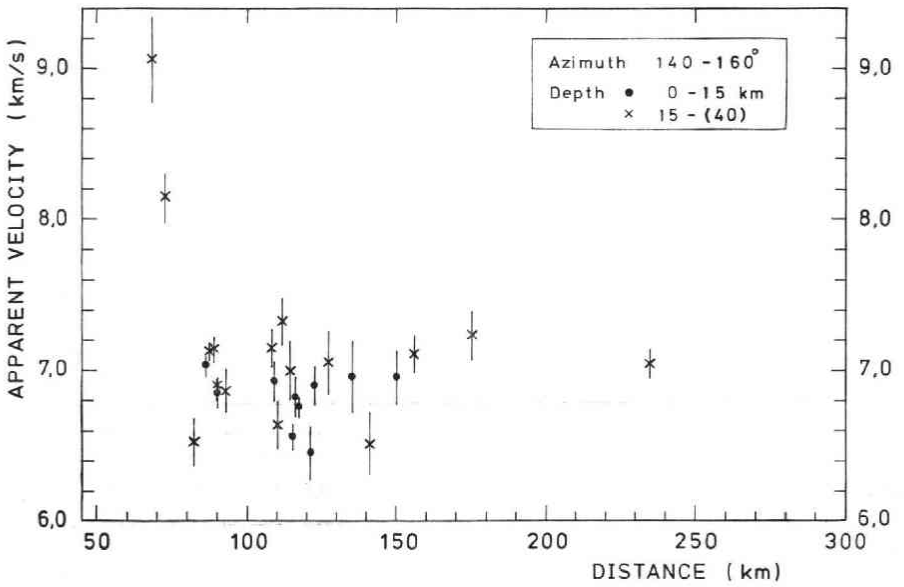

Fig. 15 (k)

and that of the latter is 15°. 3), and the peicentral distance is 200 km. The apparent velocities are distributed within 6.6–7.3 km/s and are less than the expected velocity of P_n (7.5 km/s or 8.1 km/s).

Under the velocity structure mentioned above the apparent velocity of 7.3 km/s corresponds to a depth of about 80 km beneath the trench. Therefore it seems that

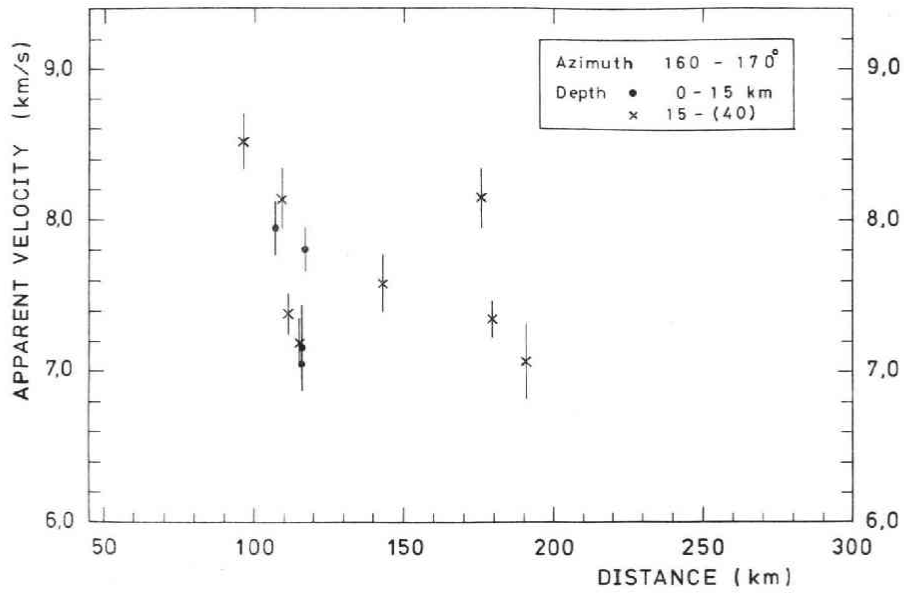

Fig. 15 (1)

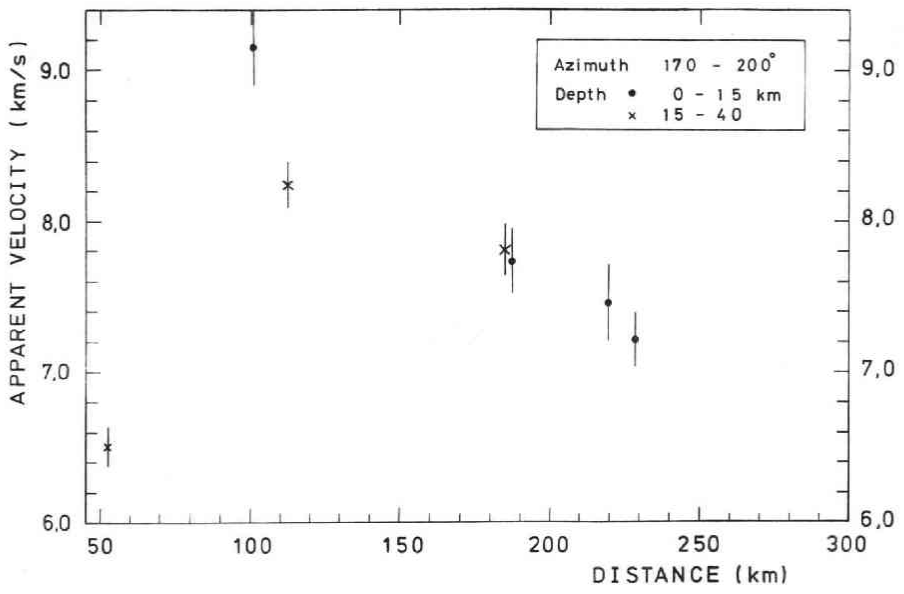

Fig. 15 (m)

the depths of the earthquakes which occurred in and around the trench were determined to be too deep by the seismic network of Tôhoku University as pointed out by Yamamoto and Kono (1976), even though the obtained apparent velocities were affected by the velocity structure. The hypocenters of earthquakes that occurred in and around the trench were relocated by Hasegawa and Umino (1978) using the data from the seismic

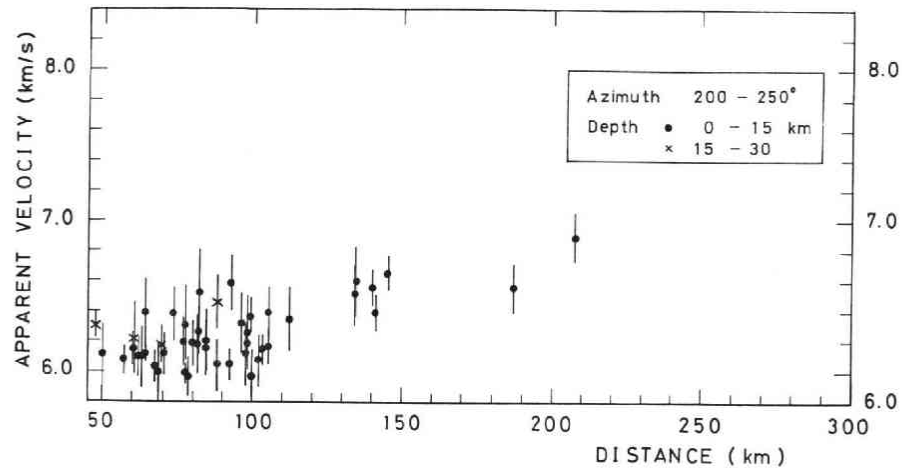

Fig. 15 (n)

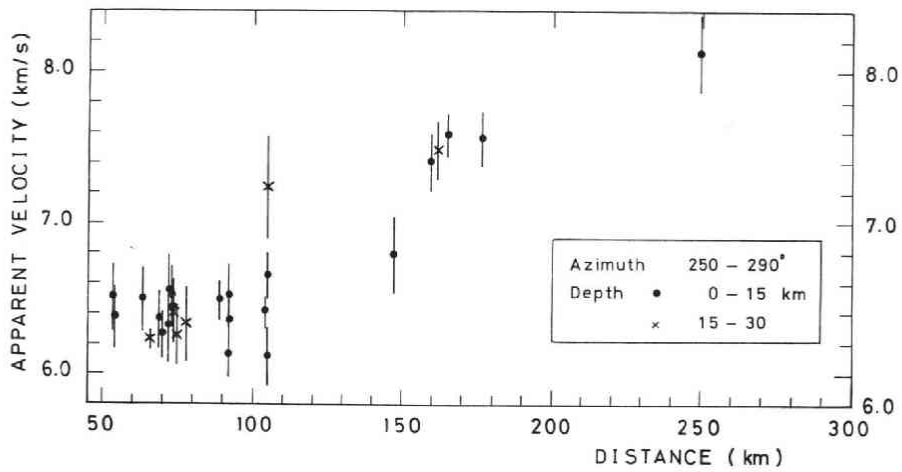

Fig. 15 (o)

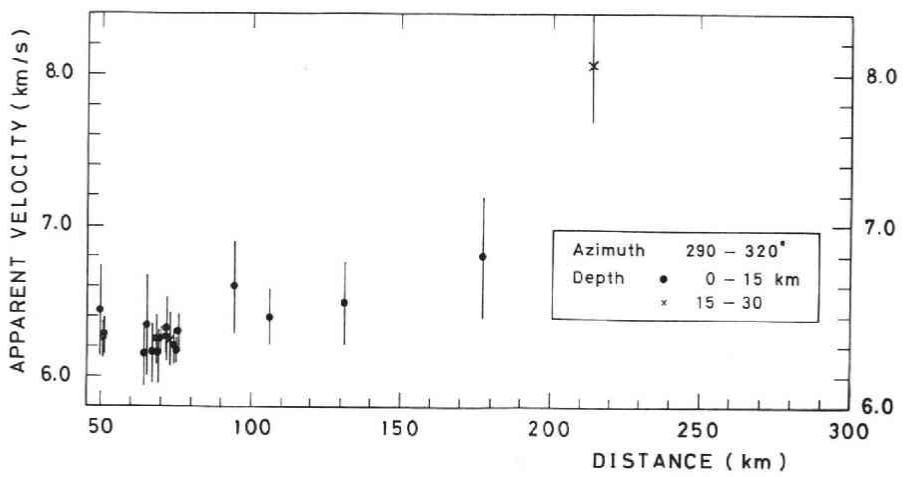

Fig. 15 (p)

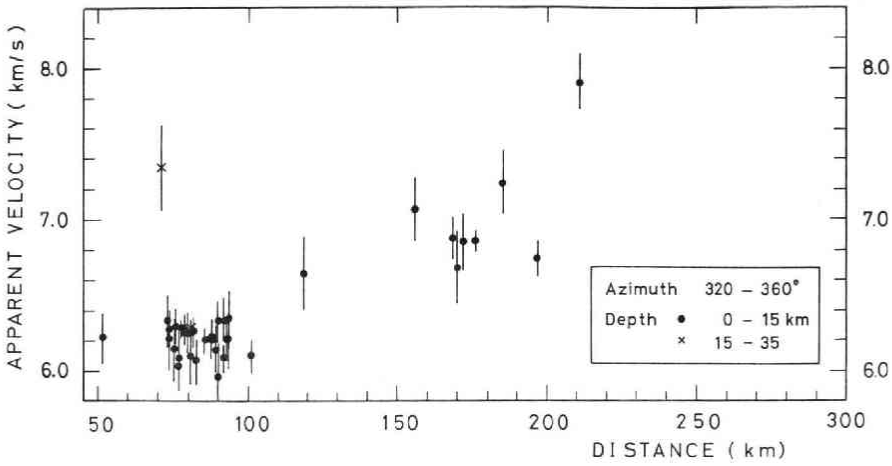

Fig. 15 (q)

Fig. 15 (a)-(q). Apparent velocities versus epicentral distances. The vertical bars indicate the standard deviations of apparent velocities. If a number showing a depth is in brackets and an epicentral distance is greater than 150 km, the depth range is extended to 60 km.

network of Tôhoku University, three stations operated by Hokkaido University in southern Hokkaido, and two temporal stations set up by Hirosaki University and Tôhoku University in Aomori Prefecture. As compared the relocated hypocenters with those determined routinely by the seismic network of Tôhoku University, both epicenters are almost the same but the depths which had been determined to be 100 km or more by the data from the seismic network of Tôhoku University were redetermined to be about 50 km or less. Nagumo *et al.* (1978), Kasahara *et al.* (1978), and Ichikawa (1979) also pointed out that the focal depths of earthquakes that occurred in and around the trench were determined to be deeper than the true depths.

3.6. *Azimuth anomalies*

The relations between the azimuth anomalies and the directions to epicenter in each 10 km depth interval are shown in Fig. 17(a)-(f). The symbols correspond the epicentral distance ranges. In the case of the epicentral distances from 150 to 200 km, the earthquakes that occurred in the east side of the array were excluded, because the accuracy of those depths is not good for the classification of every 10 km depth range.

In the case of the earthquakes whose depths are shallower than 20 km (Fig. 17(a) and(b)) there is a marked difference in patterns of the azimuth anomalies between the east side of the array (Pacific Ocean side) and the west side (the inland area). In the east side the signs of the azimuth anomalies change from positive to negative around 90–100°. On the other hand, in the west side no remarkable tendency can be seen. The patterns of the azimuth anomaly in the east side (the 20–60 km depth range) have nearly the same tendency as the cases of shallower than 20 km (Fig. 17(c)-(f)) the azimuth anomalies change abruptly around 30–40°. In the azimuth range 40–70°,

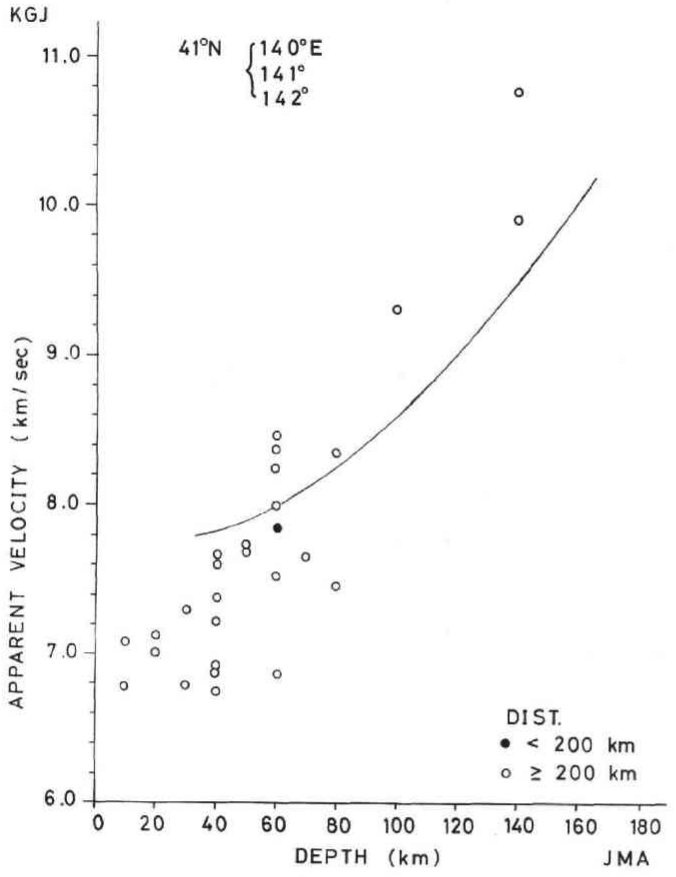

Fig. 16(a). Apparent velocities versus focal depths. The solid line represents the expected values of $d\Delta/dT$ obtained from the velocity structure adopted by the seismic network of Tôhoku University at the epicentral distance of 200 km. The region: (41–42°N, 140–143°E), the depths were determined by JMA.

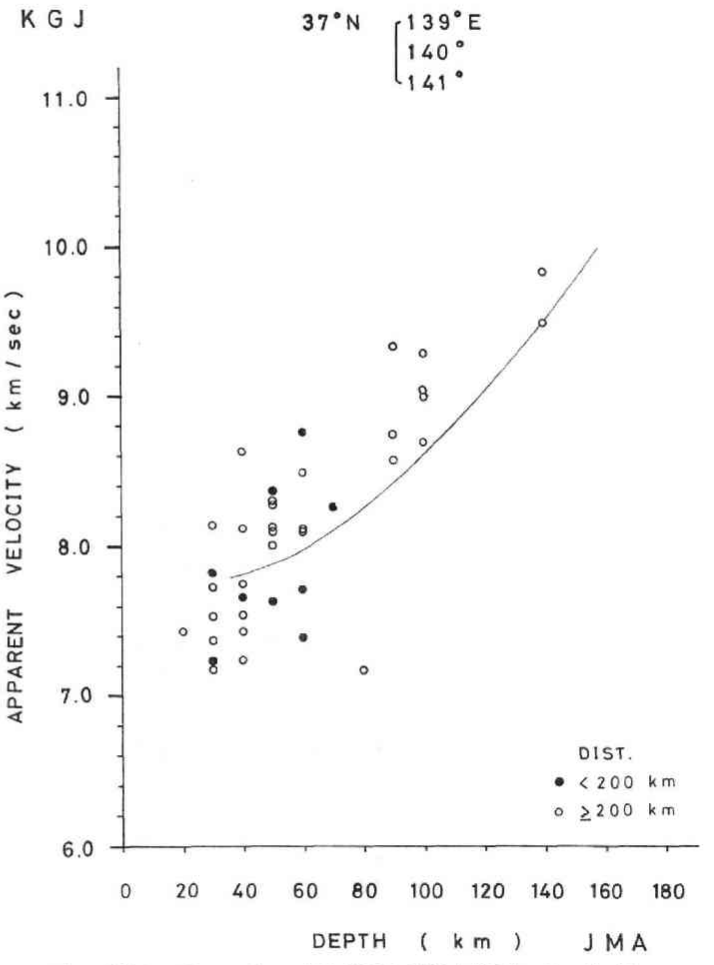

Fig. 16(b). The region: (37–38°N, 139–142°E), the depths were determined by JMA.

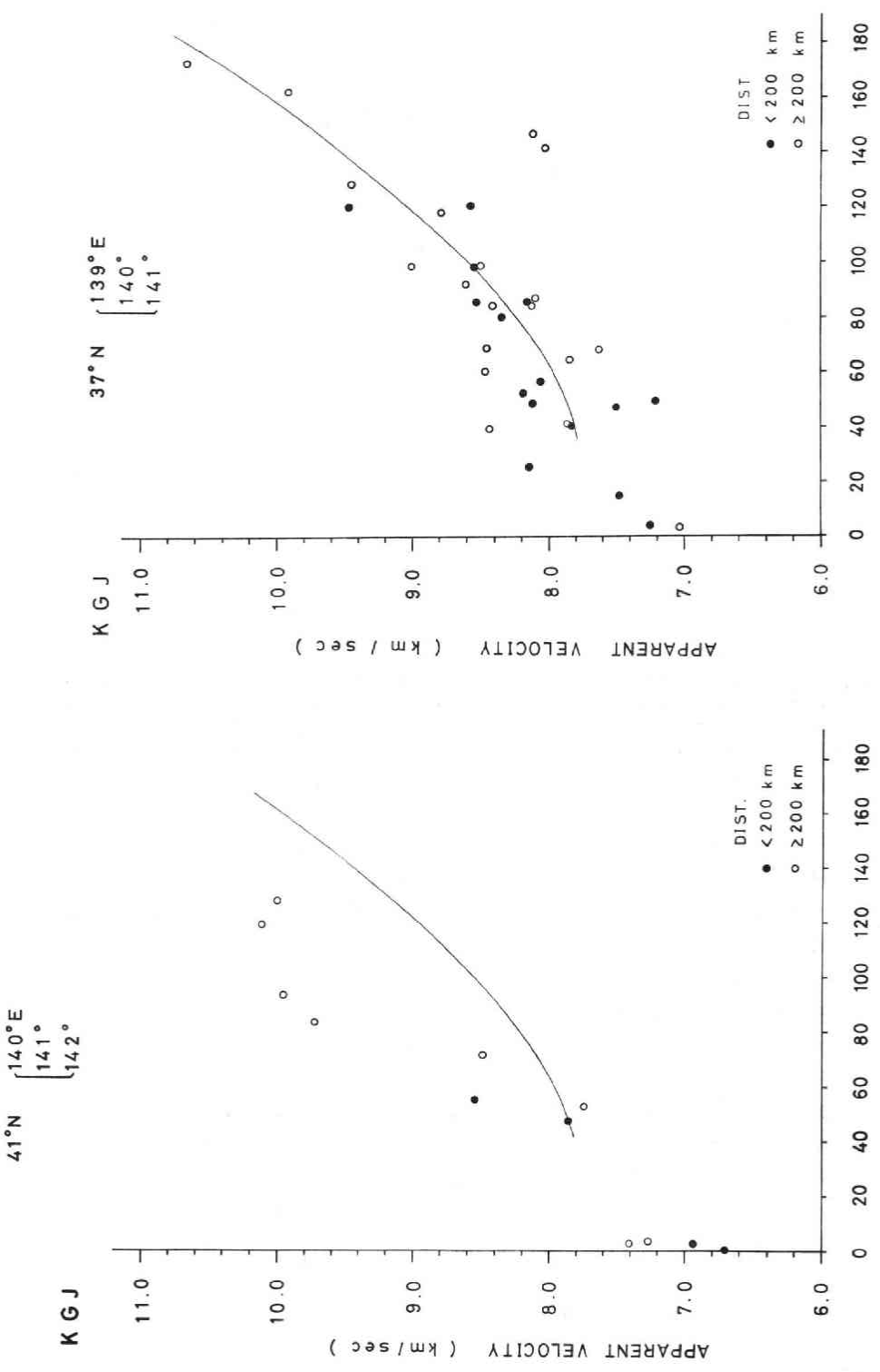

Fig. 16(c). The region: (41–42°N, 140–143°E), the depths were determined by the seismic network of Tôhoku University (NET).

Fig. 16(d). The region: (37–38°N, 139–142°E), the depths were determined by the seismic network of Tôhoku University (NET).

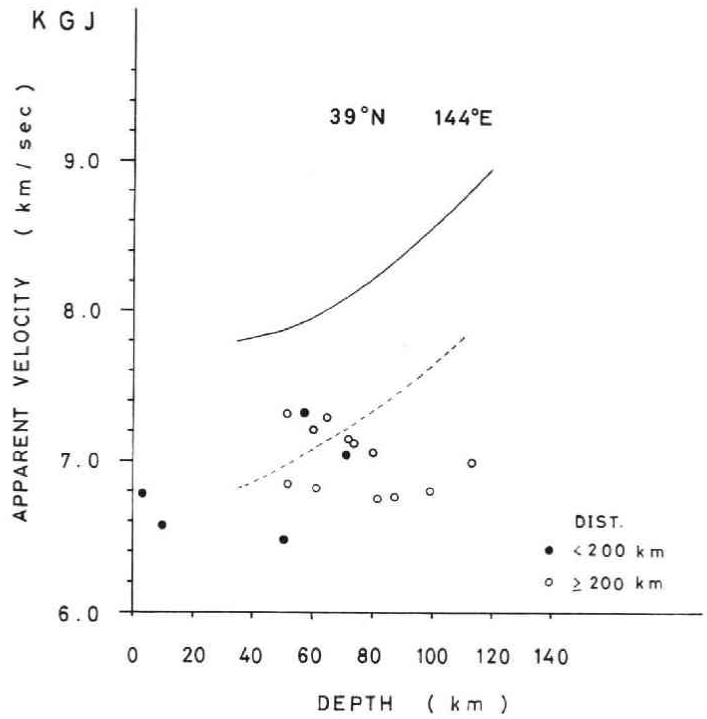

Fig. 16(e). The region: (39–40°N, 144–145°E), the depths were determined by the seismic network of Tôhoku University (NET). The dotted line is the apparent velocities at the epicentral distance of 200 km when considering that the dip directions of the Conrad (the 5.9 km/s layer– the 6.6 km/s layer) and the Moho (the 6.6 km/s layer–7.5 km/s layer) are N90°W and their dip angles are 5° and 15°, respectively (Yamamoto and Kono (1976)).

more than 10° azimuth anomalies exist. As a general tendency, however, in the azimuth range 0–30° there are no remarkable azimuth anomalies.

The average azimuth anomalies and their standard deviations were obtained under the following condition: More than 4 earthquakes occurred in an area ($0.1°\times0.1°$) over 10 km depth range and the directions of wave approach of corresponding earthquakes do not scatter. The values of the tangential distance deviations of epicenters corresponding to the azimuth anomalies were estimated for the earthquakes whose average azimuth anomalies were calculated at the average epicentral distances. Those values are given by $\bar{L}\tan d_{\varphi}$, where $\bar{L}$ is an average epicentral distance and $\overline{d_{\varphi}}$ is an average azimuth anomaly. Taking account of these tangential distance deviations of epicenters the relation between the average azimuth anomalies and the averge directions to epicenter is shown in Fig. 18. Within the accuracy of hypocenter and the standard deviations in the direction of wave approach it is thought that the earthquakes shown by the open triangles have no azimuth anomalies. It can be considered that in the azimuth range 210–0–30° there are little azimuth anomalies. The general tendency of the azimuth anomalies is positive in the north-eastern region and is negative in the south-eastern region.

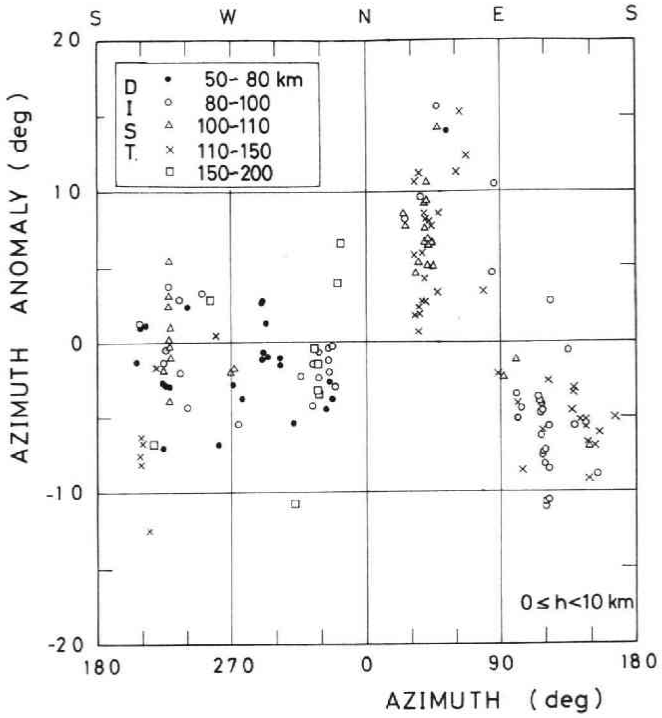

Fig. 17 (a)

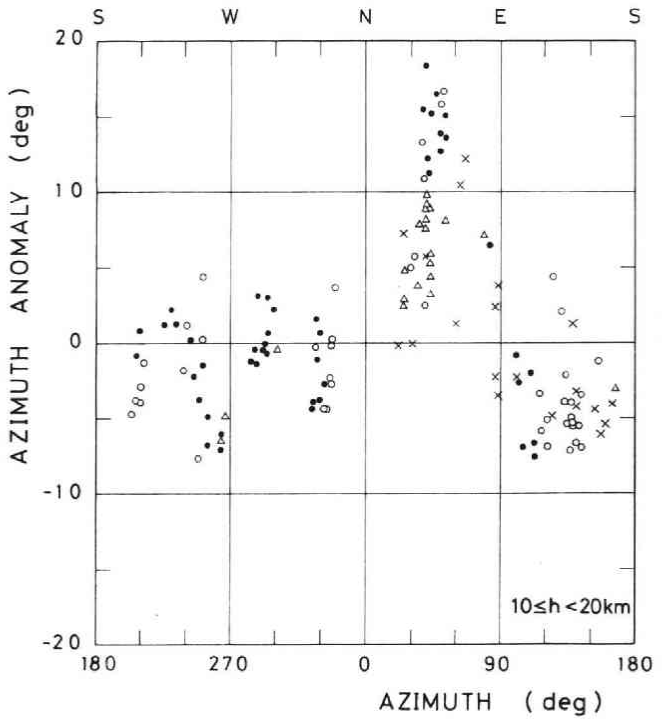

Fig. 17 (b)

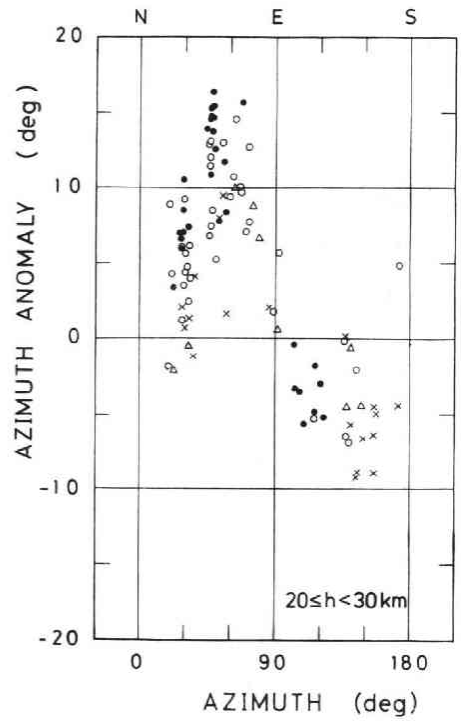

Fig. 17 (c)

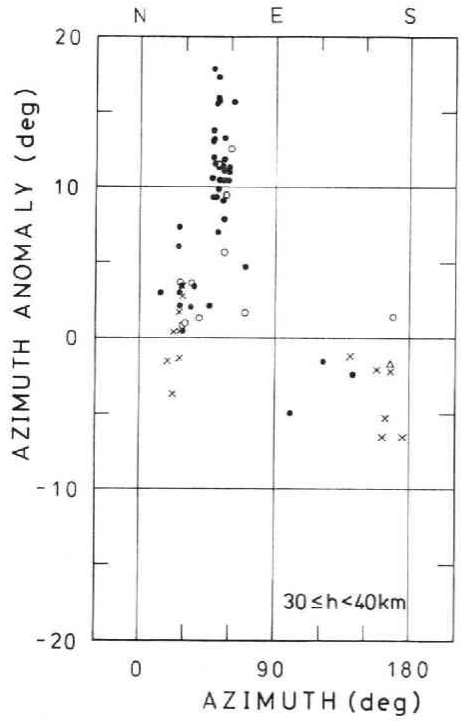

Fig. 17 (d)

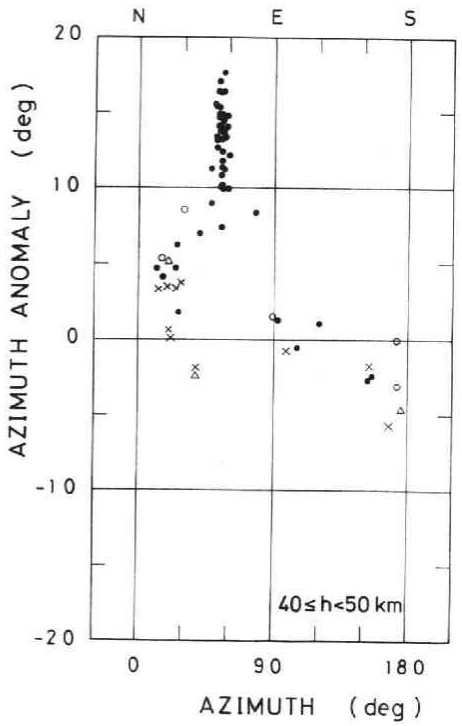

Fig. 17 (e)

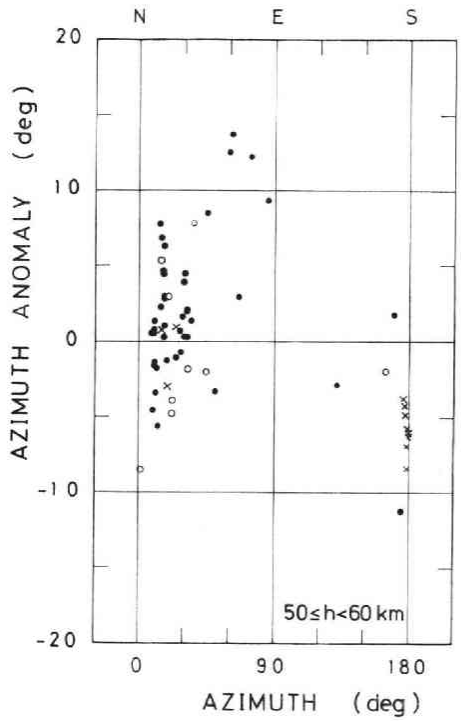

Fig. 17 (f)

Fig. 17 (a)-(f). Azimuth anomalies versus directions to epicenter. h indicates a focal depth.

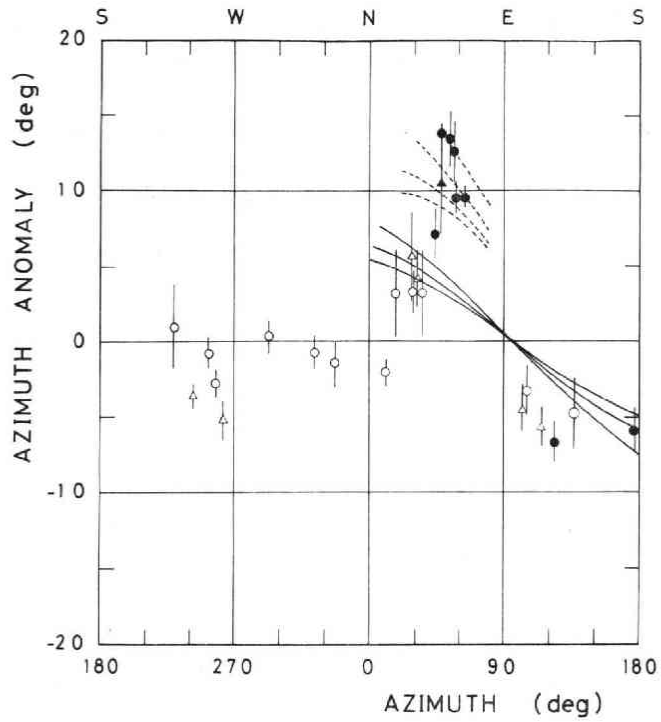

Fig. 18. The average azimuth anomalies versus the average directions to epicenter. Open circles: $0 \leqq l < 5$ km, open triangles: $5 \leqq l < 10$ km, solid cricles: $10 \leqq l < 15$ km, solid triangles: $15 \leqq l < 20$ km; $l = \bar{L} \tan \overline{d\phi}$, where $\bar{L}$ is an average epicenral distance and $\overline{d\phi}$ is an average azimuth anomaly. The vertical bars are the standard deviations of the azimuth anomlies. The solid and dotted lines represent the maximum azimuth anomalies under the velocity structures mentioned in the captions of Figs. 13 and 14.

3.7. *Apparent velocities and azimuth anomalies of the earthquakes which occurred in the deep seismic zone*

It has been pointed out by Umino and Hasegawa (1975) and Hasegawa *et al.* (1978 a) that the deep seismic zone has a double-planed structure in the Tohoku district. The earthquakes that occurred in the upper plane and those having occurred in the lower plane were separately investigated. Taking account of the dip direction of the deep seismic planes (dipping westward), the relations classified by the azimuth range between apparent velocities and epicentral distances are shown in Fig. 19(a)-(g). The azimuth range 250–290° is nearly the same as the dip direction of the deep seismic planes (Fig. 19(a) and (b)). The apparent velocities corresponding to the upper plane of the deep seismic zone were calculated by using the velocity structure adopted by the seismic network of Tôhoku University and approximating that the deep seismic zone has the constant dip angle (30°) and the dip direction (N90°W). When the epicentral distances are more than 60 km, the apparent velocities are nearly constant (14.5–15.0 km/s).

The azimuth ranges 180–200° and 0–10° correspond to the direction of the strike

and the depth range of upper boundary of the deep seismic zone is 60–80 km (Fig. 19(c) and (d)). The azimuth range 80–100° is almost opposite to the dip direction of the deep seismic zone (Fig. 19(b)).

The azimuth anomaly of the earthquakes ($h \geqq 40$ km) having occurred in the upper plane of the deep seismic zone is shown in Fig. 20(a). The characteristic pattern exists. Namely, in the north-westerly direction (azimuth range 320–350°) the azimuth

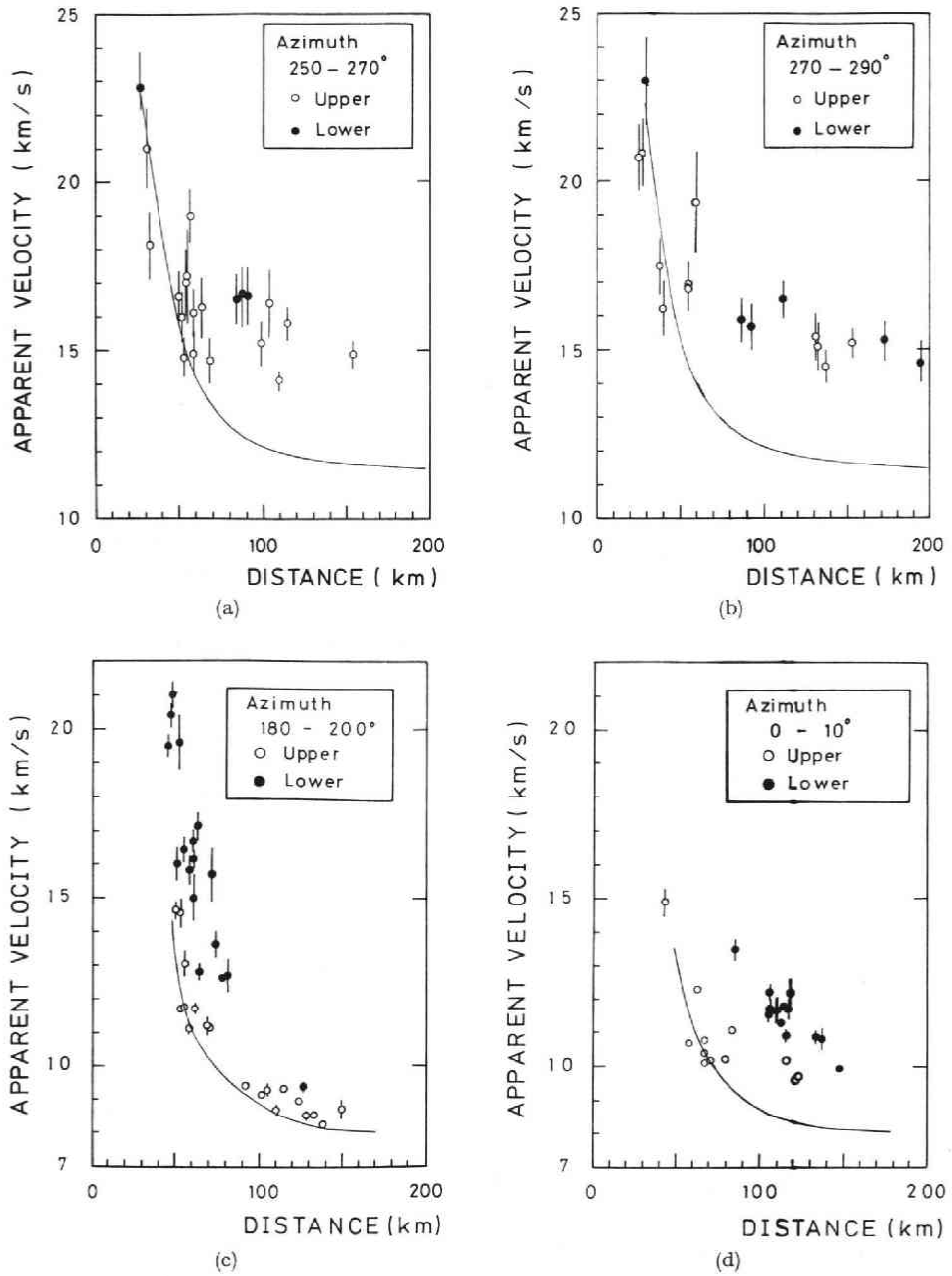

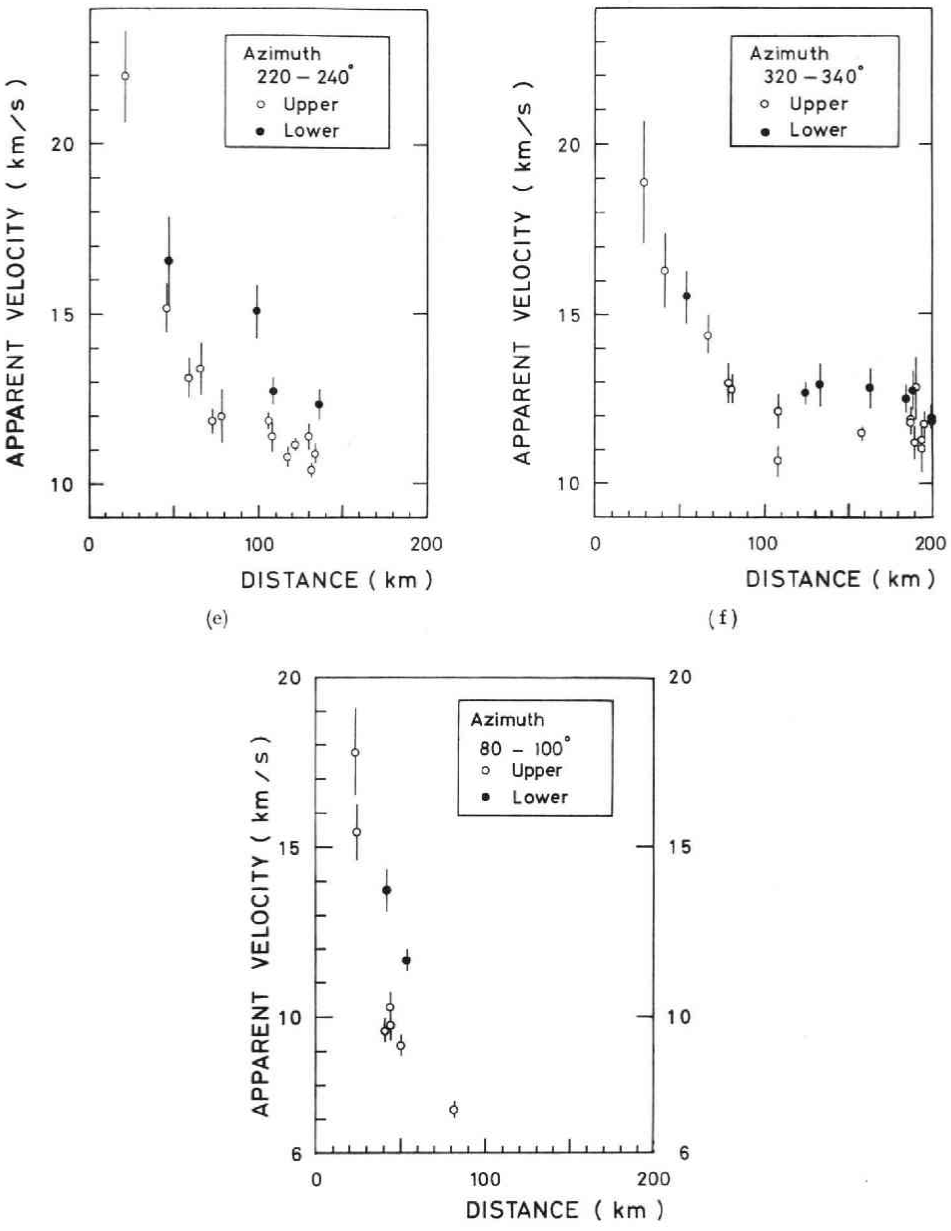

Fig. 19(a) and (b). The apparent velocities versus the epicentral distances. In the cases that the directions to epicenter is almost the same as the dip direction of the deep seismic zone. The solid line represents the expected $d\Delta/dT$ of the earthquakes that occurred at the upper boundary of the deep seismic zone from the epicentral distances, the depths and the velocity structure adopted by the seismic network of Tôhoku University.
(c) and (d). In the cases that the directions to epicenter is nearly the same as the strike of the deep seismic zone. The solid line represents the expected $d\Delta/dT$ (the focal depths were fixed at 70 km).
(e) and (f). In the cases that the directions to epicenter are between the dip direction of the deep seismic zone and its strike.
(g): In the case that the directions to epicenter are opposite to the dip direction of the deep seismic zone.

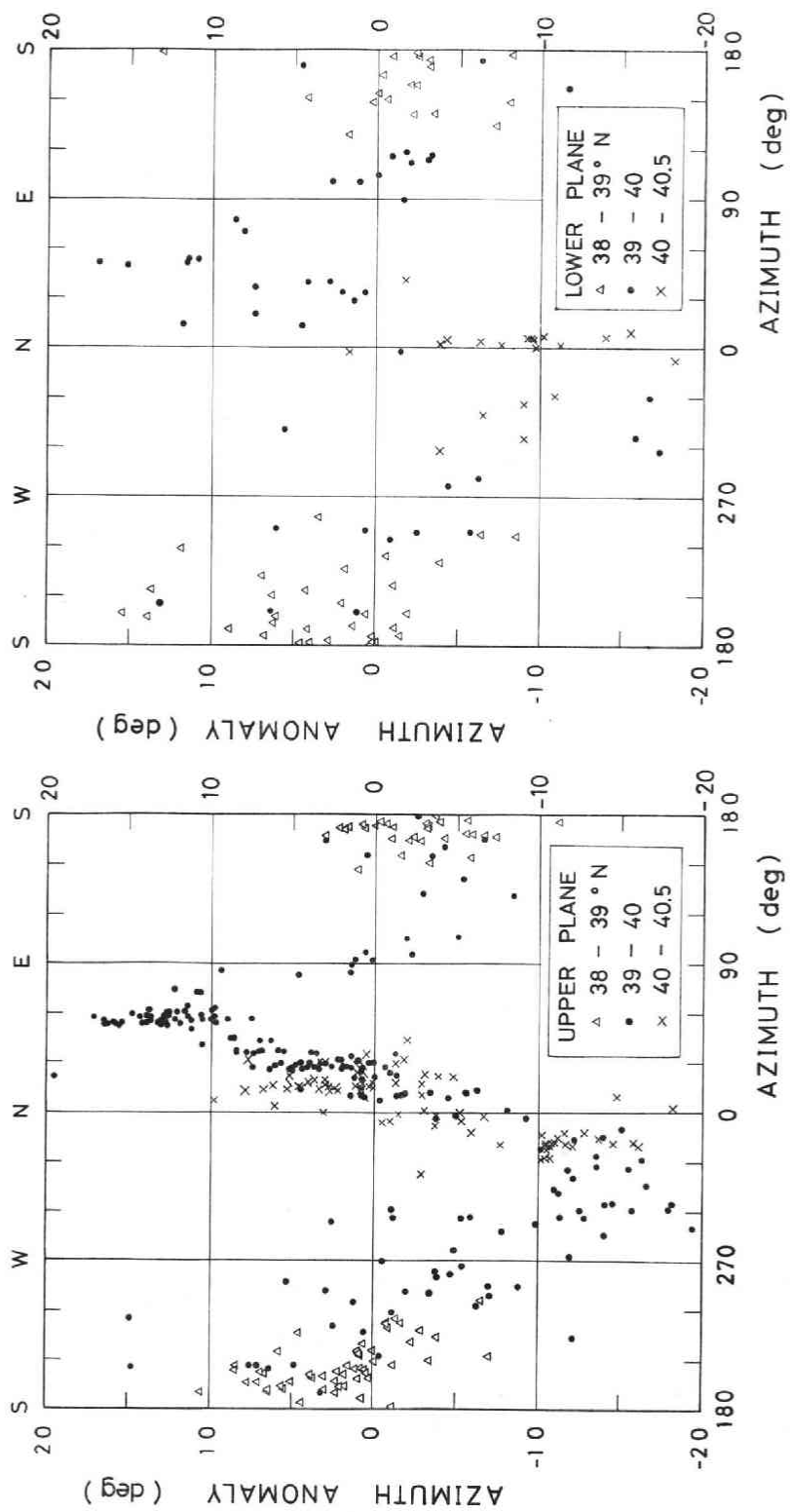

(a) (b)

Fig. 20. The azimuth anomalies of the deep earthquakes occurred (a) in the upper plane ($h \geqq 40$ km) and (b) in the lower plane ($h \geqq 40$ km).

anomalies are around $-12°$ and in the north-easterly direction (50–60°) they are around $+12°$. These large azimuth anomalies correspond to the tangential distance deviations of 10–20 km. The case of the earthquakes that occurred in the lowr plane is shown in Fig. 20(b). Compared with the case of the upper plane, the azimuth anomalies in the case of the lower plane scatter. However, the pattern of the azimuth anomalies is similar to each other.

4. Velocity structures and discussions

4.1. *Velocity structures and passing regions of seismic waves*

As mentioned above, the velocity of the granitic layer beneath the KGJ-array is 5.9 km/s. But the thickness is not given. Taking into account the velocity structure along the Oga-Kesennuma line by Yoshii and Asano (1972), a three horizontally layered structure was assumed. The velocities and the thicknesses are (5.9 km/s, 10 km), (6.6 km/s, 20 km), and (7.5 km/s, ∞), respectively. If a first arrival is P*, a seismic wave reaching a station refracts from the 6.6 km/s layer to the 5.9 km/s at a point which is about 20 km from the station. In the case of P_n a seismic wave refracts to the 6.6 km/s layer at the Moho about 50 km apart from a station and does from the 6.6 km/s layer to the 5.9 km/s layer at a point which is about 12 km from the station. When approximating that the apperture of the array is 20 km in Fig. 21 the region illustrated by ▥ is the area where P* refracts from the 6.6 km/s layer to the 5.9 km/s layer and the region with ▤ is the area where P_n refracts from the mantle to the crust. In the outside area of the largest circle in Fig. 21 we cannot get any information as to the configuration of the Moho. As the interface between the 5.9 km/s layer and the 6.6 km/s

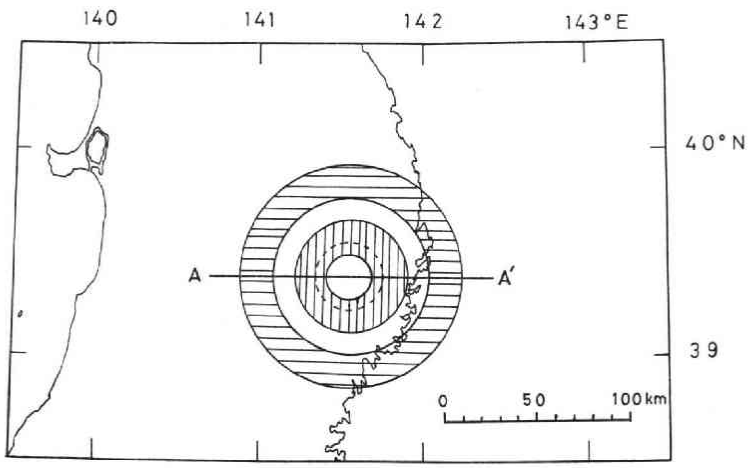

Fig. 21. Assuming a horizontally three-layered structure (5.9 km/s, 10 km thick; 6.6 im/s, 20 km thick; 7.5 km/s, ∞) and assuming that the diameter of the array is 20 km, ▥ indicates the region where P* refracts to the 5.9 km/s layer, and ▤ represents the region where P_n refracts to the 6.6 km/s layer. The dotted circle shows the outer boundary where the seismic ray with an apparent velocity of 14.0 km/s refracts to the 5.9 km/s layer.

layer (the Conrad (discontinuity)) we can obtain some information on the inside area of the second smallest circle in Fig. 21. As mentioned above, the regions where waves approaching to the array propagate are extremely limited. Therefore it should be emphasized that the apparent velocities and the directions of wave approach obtained from the array observations are directly and strongly affected by the local structure beneath the array and its adjacent region.

4.2. *Azimuth anomalies, velocity anomalies, and dipping structures*

When the sources of the azimuth and velocity anomalies are dipping interfaces the general relations between the velocity structures and the azimuth and velocity anomalies are given in the following. The patterns of the azimuth anomalies and those of the apparent velocities depending on the dipping interface(s) were shown in Fig. 9(a) and (b). The perpendicular direction against the azimuth where the sign of the azimuth anomaly changes is the strike of the dipping interface, that is, the direction with addition of 180° against the azimuth where the sign of the azimuth anomaly changes from positive to negative is the dip direction. On the other hand, the azimuth where the apparent velocity of the specified phase (*e.g.* P_n) has a maximum value is the dip direction, namely, the azimuth with 90° addition against the azimuth where the apparent velocity of that phase reaches a minimum value is the strike direction. The dip angle of the dipping interface can be determined by calculating the angle which satisfies the quantity of apparent velocity and azimuth anomaly.

4.3. *Velocity structures in the east side of the array*

In Fig. 17(a)–(f) the patterns of the azimuth anomalies are almost similar in the depth range 0–60 km. This means that the structures of the shallower part mainly contribute to the azimuth anomalies. The signs of the azimuth anomalies change from positive to negative around 90–100° (Fig. 17(a)-(f)). The apparent velocities have minimum values around the same azimuth range (Figs. 13(a)-(c), and 14). The azimuth range 90–100° satisfies the conditions of the azimuth with addition of 180° against the dip direction. Therefore the interfaces dipping to the west are expected. From the relations between apparent velocities and epicentral distances in the azimuth ranges 80–100° and 100–120° (Fig. 15(h) and (i)), we obtain

Epicentral distance	Focal depth	Apparent velocity
– 90 km	0–15 km	6.3–6.4 km/s
100–170	0–40	6.4–7.1
180–	0–	6.8–7.2

In the case of the earthquakes with epicentral distances of less than 90 km it can be thought that a seismic wave which passes in the 6.6 km/s layer reaches the array as a first arrival. Therefore we consider that the apparent velocity is changed from 6.6 km/s to 6.3 km/s by the dipping Conrad discontinuity.

When taking into account the velocity structure of the oceanic crust and mantle

derived by Yoshii and Asano (1972) the P_n phase is expected to be a first arrival in the distance range of more than 200 km. RGES (1977) pointed out that the boundary of the P_n velocity where the value of P_n changes from 8.1 km/s (oceanic) to 7.5 km/s (continental) almost coincides with the aseismic front proposed by Yoshii (1975). The expected apparent velocity of P_n (*i.e.* 8.1 km/s or 7.5 km/s) depends on the positions of the boundary between the oceanic mantle and the continental mantle (OM–CM boundary) and the array. Let us consider the effects of the OM-CM boundary to the apparent velocities. It is assumed that the dip angle of the OM-CM boundary is 90° (vertical) and the strike is in the north-south direction. If the incident angles of seismic waves at the OM-CM boundary is less than 15° (*i.e.* the angle between the vertical line and the seismic rays are 90–75°), the effects for the z-components of the direction vector of the seismic rays are small (less than 1%). Therefore the effects of the OM-CM boundary on the apparent velocities are negligible. As to the P_n phase we consider two interfaces (*i.e.* the Conrad and the Moho) which contribute to the anomalies of apparent velocities. In the part of the interface between the 5.9 km/s layer and the 6.6. km/s layer where the P* phases which reach the array pass the dip angle of the interface was determined to be 7° by using equation (3). The dip angle of the Conrad where the P_n phase reaching the array passes was assumed to be also 7°, though the part of the Conrad where the P_n phase passes is nearer to the central station of the array than the case of the P* phase. It is likely that the dip direction of the Moho agrees with that of the Conrad because the azimuths where the signs of the azimuth anomalies change are independent of the focal depth range 0–60 km. When the P_n velocity is 7.5 km/s, the dip angle of the Moho is 11°. The dip angles of 7° and 11° give the vertical differences of about 1.2 km and about 1.9 km for a 10 km horizontal distance, respectively. As for the velocity structure which can explain both the lowest values of the apparent velocities and the change of the sign of azimuth anomalies from positive to negative at a azimuth of about 85°, it should be noted that the Conrad has a dip angle of 7° and a dip direction of N85°W, and that the Moho has a dip angle of 11° and the same dip direction as the Conrad. Assuming that this velocity structure exists in the east side of the array the apparent velocities of P* and P_n are calculated and are shown in Fig. 13(a), (b), and (c). In Fig. 14 the dotted lines indicate the calculated apparent velocities of P_n in the case of the velocity structure mentioned above and the angles between the incident seismic rays and the perpendicular lines are 90° (lower) and 80° (upper), respectively. The azimuth anomalies (maximum values) under the same velocity structure are shown in Fig. 18 with solid lines. In the south-east side of the array it seems that the velocity structure is generally the same as that of the azimuth range 80–100°. In the azimuth range 40–70° the azimuth anomalies are large (10–15°) in the depth range 0–60 km. These large azimuth anomalies are considered to be caused by the structure of the Moho and the Conrad, because the azimuth anomalies are almost independent of the focal depths. In the present study the OM-CM boundary is not taken into consideration. In this azimuth range the apparent velocity corresponding to the 6.6 km/s layer is 6.5 km/s

(Fig. 15(d) and (e)) and that corresponding to the P_n velocity is 7.0–7.5 km/s (Fig. 14). The apparent velocities with the epicentral distance range 50–60 km and with the depth range 40–50 km are 8.5–9.2 km/s (Fig. 13(e)). The apparent velocities expected from the velocity structure adopted by the seismic network of Tôhoku University are about 9.0±0.5 km/s in the region of interest. Using the same analysis as in the case of the azimuth range 80–120°, the dip direction of the Conrad and that of the Moho are N50°W and their dip angles are about 15° and 20°, respectively. Takahashi (1982) obtained that the dip angle of the Moho in and around Miyako corresponding to the azimuth range 40–70° is about 15–20° by analyzing the data from the S to P converted waves at the Moho. Our result is in good agreement with his result. In this azimuth range 40–70° the earthquakes which occurred in an around Miyako have large and positive azimuth anomalies. Hasegawa *et al.* (1976) pointed out that the aseismic front enters the inland around Miyako and there is the folding structure of the deep seismic plane which extends from off Miyako to the central Tohoku district (the northeast-southwest direction) and that the folding structure is remarkable around Miyako. Takagi *et al.* (1973) showed that the earthquakes that occurred in and around Miyako do not have the east-west pressure axes which surpass in and around the Tohoku district and have complex focal mechanisms. Ishii (1977) found the north-south compression at Miyako and the east-west compression at the other stations (Sanriku, Himekami, Nibetsu, and Oga) in the Tohoku district. Therefore it appears that the structure and the earthquake generating stress field are very complex in and around Miyako.

4.4. *Velocity structures in the west side of the array*

In the west side there are no large azimuth anomalies over a wide range. In the azimuth range 200–250° the jump of the lowest apparent velocities can be seen around the epicentral distance of 120 km (Fig. 15(n)). The lowest apparent velocity of epicentral ditance range less than 120 km is about 5.9 km/s and that of more than 120 km is about 6.5 km/s. In the epicentral distance range less than 80 km and in the azimuth range 290–320° the slowest apparent velocity is about 6.1 km/s (Fig. 15(p)) and in the azimuth range 320–360° that is about 6.0 km/s (Fig. 15(q)). In the azimuth range 250–290° the slowest apparent velocity seems to be 6.0 km/s but it is not clear. In the epicentral distance range 100–150 km the data on the apparent velocities are not enough in quantity except for the azimuth range 200–250°. Therefore the slowest apparent velocity in this epicentral distance range cannot be determined. However that can be presumed to be about 6.5 km/s from Fig. 15(p).

The apparent velocities of the four earthquakes which occurred in the azimuth range 250–290° and in the epicentral distance range 160–180 km are 7.4–7.6 km/s (Fig. 15(o)). Their first arrivals are considered as P_n. Those values (7.4–7.6 km/s) coincide with the velocity of P_n under the Kesennuma-Oga profile (in the north-eastern Japan) with 7.53±0.05 km/s obtained by RGES (1977). On the other hand, the apparent velocities of the earthquakes which occurred near Mt. Iwaki (in Aomori Prefecture) and have about the same epicentral disrances but different azimuths are 6.8–6.9 km/s

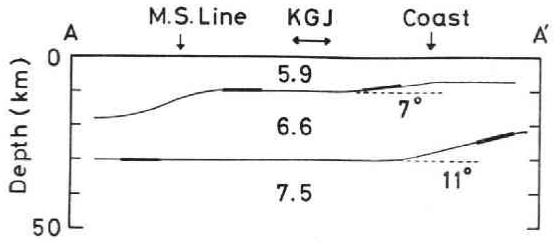

Fig. 22. Velocity structure model along the A-A′ cross section (the east-west direction, Fig. 21). The thicknesses of the 5.9 km/s layer and the 6.6 km/s layer are assumed to be 10 and 20 km rightly under the array, respectively. The dip angles were determined with the azimuth anomalies and the apparent velocities which were obtained from the data of the seimic waves that can pass through the thick parts of the lines showing the interfaces. The M.S. line is the Morioka–Shirakwa tectonic line. The shape of the bottom of the 5.9 km/s layer at and around the M.S. line is based on the result of Yoshii and Asano (1972).

(Fig. 15(q)). In the Fig. 15(q) (azimuth range 320–360°) there is only one earthquake indicated by the cross, which occurred just under the Mt. Iwate (volcano). The epicentral distance is 71 km, the depth 31.6 km, and the apparent velocity is 7.3 km/s. If the first arrivals of the earthquakes beneath Mt. Iwaki are P_n their apparent velocities are expected to be almost the same as the apparent velocity of the earthquake occurred rightly under Mt. Iwate, because they have almost same azimuth. But the observed apparent velocities of the earthquakes occurred near Mt. Iwaki are 6.8–6.9 km/s and are smaller than that of under Mt. Iwate (7.3 km/s). It is considered that the first arrivals of the former are affected by the velocity structure under Mt. Iwate and the other volcanoes.

From this subsection and the preceding subsections, a simplified velocity structure of the A-A′ cross section (Fig. 21, the east-west direction) is shown in Fig. 22 as an example. The thicknesses of the 5.9 km/s layer and the 6.6 km/s layer are assumed to be 10 and 20 km beneath the array, respectively. The dip angles were determined with the data given by the seismic waves which pass through the thicker parts of the lines showing the interfaces. The M.S. line means the Morioka-Shirakawa tectonic line. The shape of the Conrad around the M.S. line is based on the result presented by Yoshii and Asano (1972).

4.5. *Apparent velocities and azimuh anomalies of the deep earthquakes*

The apparent velocities of the earthquakes with the epicentral distance range of more than 60 km are nearly constant (14.5–15.0 km/s) in the azimuth range of 250–290° which is nearly the same as the dip direction of the deep seismic zone (Fig. 19(a) and (b)). In the case that the hypocenters determined by using the apparent velocities are plotted on the east-west cross section the deep seismic zone becomes steeper near 141°E (Yamamoto and Kono (1975)). Hasegawa *et al.* (1978b) explained this bending by considering the slab which has a dip angle of 30° and the 6% faster velocity than the surrounding mantle. It is considered that the P waves of the deep earthquakes

occurred in the west side of 141°E pass the inside of the slab (high V and high Q) up to 141°E and reach the array.

The azimuth anomalies are large negative values in the azimuth range 300–350° and large positive ones in the azimuth range 50–60° (Fig. 20(a) and (b)). The epicentral distribution given by Hasegawa *et al.* (1978b) shows that the explanation for the azimuth anomalies is difficult even if the slab mentioned above is taken into consideration. In the azimuth range 40–70° the depths of the earthquakes occurred in the deep seismic zone are 40–50 km. The sources of the azimuth anomalies of the earthquakes occurred in this region (depth range 0–60 km), as we mentioned in subsection 4.3., are considered to be the westward dipping of the Conrad (dip direction N50°W, dip angle about 15°) and the Moho (dip direction N50°W, dip angle about 20°). The large negative azimuth anomalies in the north-west cannot be explained by the shape of the deep seismic zone itself even if simple irregularities of the deep seismic zone are taken into consideration. The Conrad and the Moho are almost flat in this azimuth range (see subsection 4.4), therefore they cannot cause those large azimuth anomalies.

5. Conclusions

The investigation of the apparent velocities, azimuth anomalies, and the velocity structures was made on the basis of the data from the Kitakami seismic array and the seismic network of Tôhoku University. The following results are obtained:

1) The velocity of the granitic layer beneath the KGJ-array is 5.9 km/s.

2) Under the Japan trench (off the Sanriku coast) and its vicinity no earthquakes with an apparent velocity of more than 7.4 km/s were observed. Therefore it is considered that the depths of the earthquakes having occurred in and around the trench are not more than 100 km.

3) In and around the Sanriku coast (in azimuth range 80–120°) the Conrad and the Moho have the same dip direction (N85°W) and their dip angles are 7° and 11°, respectively.

4) Near Miyako the Conrad and the Moho have the same dip direction (N50°W) and their dip angles are about 15° and about 20°, respectively.

5) In the west side of the array (the inland area) the Conrad is almost flat. In the azimuth range 260–270° the Moho is nearly flat. In the other azimuth ranges it is impossible to discuss the shape of the Moho because no P_n phase was observed.

6) The large and negative azimuth anomalies of the deep earthquakes occurred in the north-west direction of the array cannot be explained by the down-going slab (the dip angle is about 30°, the dip direction about N70°W, and the velocity is 6% more than the mantle).

Acknowledgements: The authors would like to express their appreciation to Prof. Z. Suzuki for his guidance and encouragement during this work, and also to Prof. A. Takagi and Prof. T. Hirasawa for their suggestions and discussions. Thanks are also due to Dr. H. Hamaguchi in Geophysical Institute, Dr. H. Ishii, Dr. A. Hasegawa, and

the other members of Observation Center for Earthquake Prediction, Geophysical Observatories, and Seismological Observatories, Faculty of Science, Tôhoku University for their helpful discussions.

References

Hasegawa, A. and N. Umino, 1978: Hypocentral distribution and focal mechanisms in the northeastern Japan, *Abstract, Annual Meeting, Seismological Society of Japan, 1978*, No. 1, 34 (in Japanese).

Hasegawa, A., N. Umino, and A. Takagi, 1978 a: Double-planed structure of the deep seismic zone in the northeastern Japan arc, *Tectonophysics*, **46**, 43–58.

Hasegawa, A., N. Umino, and A. Takagi, 1978 b: Double-planed deep seismic zone and upper mantle structure in the northeastern Japan arc, *Geophys. J.R, astr. Soc.*, **54**, 281–296.

Ichikawa, M., 1979: Determination of hypocenters of earthquakes occurring off the east coast of northern Honshu, *Kenshinjiho (Quart. J. Seismol.)*, **43**, 59–65.

Ishii, H., 1977: Characteristics of crustal movement observed at wide area, *Proceeding of Earthquake Prediction Research Symposium* (1976), 116–126 (in Japanese with English abstract).

Kasahara, J., S. Nagumo, and S. Koresawa, 1978: Seismic activity under the ocean bottom and seismic gap off Sanriku, *Abstract, Annual Meeting, Seismological Society of Japan, 1978*, No. 2, 43 (in Japanese).

Matuzawa, T., 1935: Examples of deviation of first motions of seismic waves, *Zisin (J. Seismol. Soc. Japan)*, **7**, 179–184 (in Japanese).

Mikumo, T., 1965: Determination of phase velocity and direction of wave approach from station array, *Bull. Disas. Prev. Res. Inst., Kyoto Univ.*, **15**, Part 1, No. 88, 31–43.

Nagumo, S., J. Kasahara, and S. Koresawa, 1978: Seismic activity of shallow earthquakes occurred around the seamount Erimo, Japan trench, *Abstract, Annual Meeting, Seismological Society of Japan, 1978*, No. 1, 38 (in Japanese).

Niazi, M., 1966: Corrections to apparent azimuth and travel-time gradients for a dipping Mohorovičić discontinuity, *Bull. Seism. Soc. Am.*, **56**, 491–509.

Otsuka, M., 1966: Azimuth and slowness anomalies of seismic waves measured on the central California seismographic array. Part I. Observation, *Bull. Seism. Soc. Am.*, **56**, 223–239.

Recearh Group for Explosion Seismology, 1977: Regionality of the upper mantle around northeastern Japan as derived from explosion seismic observations and its seismological implications, *Tectonophysics*, **37**, 117–130.

Sato, T., 1979: Velocity structure of the crust beneath the northeastern part of Honshu, Japan, as derived from local earthquake data, *J. Phys. Earth*, **27**, 239–253.

Suzuki, Z., A. Takagi, A. Yamamoto, and T. Kono, 1972: Preliminary report on Kitakami Seismological Observatory, *Report of the Disaster Prevention Research in Tohoku District'* **8**, 75–90 (in Japanese).

Takagi, A., A. Hasegawa, and N. Umino, 1973: Focal mechanism of the shallow earthquakes having occurred in the northeastern Japan, *Abstract, Annual Meeting, Seismological Society of Japan, 1973*, No. 1, 124 (in Japanese).

Takahashi, A., 1982: The depth of the Moho in and around the Pacific coast, northeastern Japan, M.S. Thesis, Tohoku University, Sendai.

Umino, N. and A. Hasegawa, 1975: On the two-layered structure of deep seismic plane in northeastern Japan arc, *Zisin (J. Seismol. Soc. Japan), Ser.* **2**, **27**, 125–139. (in Japanese with English abstract).

Yamamoto, A. and T. Kono, 1975: Microearthquake activity in the Tohoku district and the area off the Sanriku coast, *Abstract, Annual Meeting, Seismological Society of Japan, 1975*, No. 2, 39 (in Japanese).

Yamamoto, A. and T. Kono, 1976: Earthquakes occurred around the Japan trench, off the Sanriku coast, *Abstract, Annual Meeting, Seismologial Society of Japan, 1976*, No. 1, 19 (in Japanese).

Yoshii, T. and S. Asano, 1972: Time-term analyses of explosion seismic data, *J. Phys. Earth*, **20**, 47–57.

Yoshii, T., 1975: Proposal of the "Aseismic Front", *Zisin (J. Seismol. Soc. Japan,)*, *Ser.* **2**, **28**, 365–367 (in Japanese).